Regulation of lipid dysmetabolism and neuroinflammation linked with Alzheimer's disease through modulation of Dgat2

Archana Yadav[1], Xiaosen Ouyang[1], Morgan Barkley[1], John C Watson[1], Kishore Madamanchi[1], Josh Kramer[1], Jianhua Zhang[1, 2], Girish Melkani[1, 2]

[1]Department of Pathology, Division of Molecular and Cellular Pathology, Heersink School of Medicine, University of Alabama at Birmingham, Birmingham, AL 35294, USA. [2] UAB Nathan Shock Center, Birmingham, AL 35294

[2]Corresponding Address: Department of Pathology, Division of Molecular and Cellular Pathology, School of Medicine, University of Alabama at Birmingham, AL 35294, USA. Tel.: 1-205-996-0591; Fax: 1-205-934-7447; E-mail: girishmelkani@uabmc.edu (GCM)

Abstract

Alzheimer's disease (AD) is a progressive neurodegenerative disorder characterized by amyloid-β (Aβ) plaque accumulation, cognitive decline, lipid dysregulation, and neuroinflammation. Mutations in the Amyloid Precursor Protein (APP), and accumulation of A*β42* contribute to AD, however, underlying mechanisms linking beta amyloid to lipid metabolism and neuroinflammation remain unclear. Using *Drosophila* models, we demonstrate that App^{NLG} and *Aβ42* lead to progressive locomotor impairments, disrupted sleep activity, memory deficits, lipid dysregulation, loss of synaptic integrity, and neuroinflammation. Lipid accumulation and neuroinflammation have also been observed in the App^{NLG-F} knockin mouse model, supporting their involvement in AD pathogenesis. Furthermore, we demonstrate a role of Diacylglycerol O-acyltransferase 2 (Dgat2), a key enzyme in lipid regulation, in modulating AD phenotypes, as Dgat2 and the levels of its potential transcription factors were altered in AD Drosophila and mouse models. In App^{NLG} and *Aβ42 Drosophila* AD models, *Dgat2* knockdown reduced lipid accumulation, restored synaptic integrity, improved locomotor and cognitive function, and attenuated neuroinflammation. Additionally, Dgat2 modulation improved sleep quality and circadian rhythms, further implicating lipid metabolism in AD progression. In App^{NLG-F} mice, Dgat2 inhibition mitigated lipid dysmetabolism decreased neuroinflammatory responses, and reduced expression of AD risk genes. These findings underscore the intricate interplay between amyloid pathology, lipid dysregulation, and neuroinflammation, and suggest that targeting Dgat2 may provide a novel therapeutic strategy for mitigating AD-associated

dysfunction. Understanding the conserved impact of lipid homeostasis across species offers valuable insights into potential translational interventions for AD.

Keywords: Alzheimer's disease (AD); diacylglycerol O-acyltransferase 2; lipid metabolism; amyloid precursor protein, amyloid β; neuroinflammation, sleep, circadian rhythm, drosophila, mouse models.

Abbreviations

Dgat2: Diacylglycerol O-acyltransferase 2
Dgat2 KD: Diacylglycerol O-acyltransferase 2 knockdown
Dgat2 OE: Diacylglycerol O-acyltransferase 2 overexpression
APP: Amyloid precursor protein
Aβ: Amyloid β

Introduction

Alzheimer's disease (AD) is a progressive neurodegenerative disorder that primarily affects older adults and is the leading cause of dementia worldwide[1,2]. While the exact causes of AD are still not fully understood, genetic mutations play a significant role, especially in early-onset familial forms of the disease. Three rare single-gene variants, Amyloid Precursor Protein (APP), Presenilin1 (PSEN1), and Presenilin2 (PSEN2) are known to be responsible for these familial cases. APP encodes the amyloid-β precursor protein, which, when cleaved by enzymes such as β-secretase and γ-secretase, generates amyloid-β (Aβ). These amyloid-β molecules aggregate into plaques, a hallmark feature found in the brains of AD patients. Despite decades of research into the pathophysiology of AD, the precise molecular mechanisms driving the disease remain unclear, and there is still no effective treatment to slow or halt its progression[3-5].

One of the critical aspects of AD pathogenesis involves disturbances in lipid metabolism [6, 7]. In AD, lipid dysregulation is commonly observed, with altered lipid profiles and lipid accumulation found in both animal models and postmortem human AD brains[8]. Several lipid-related genes have been identified as genetic risk factors for AD, including Apolipoprotein E (ApoE), ABCA1 (ATP-Binding Cassette Transporter A1), PICALM

(Phosphatidylinositol-binding clathrin assembly protein), and TREM2 (Triggering receptor expressed on myeloid cells 2)[9, 10]. Notably, the ApoE ε4 allele is a well-established genetic risk factor for late-onset AD, with ApoE playing a crucial role in lipid transport and neuronal integrity[11]. The upregulation of key enzymes like fatty acid synthase (FAS) and acetyl-CoA carboxylase (ACC) in both mouse models and human AD tissue suggests a disruption in lipid synthesis that may contribute to disease progression. These changes in lipid metabolism, particularly the accumulation of palmitic acid (C16) near amyloid plaques, emphasize the potential of targeting lipid pathways for therapeutic intervention in AD[12-14]. Astrocytes are a diverse group of neural cells that primarily degrade fatty acids in the brain. Their metabolic role in AD and neurodegeneration is beginning to be understood, with recent studies suggesting that impaired astrocytic fatty acid degradation may contribute to lipid dysregulation in the brain. This dysfunction in astrocytes could represent a key mechanism driving the pathophysiology of AD. Human Eph14 knock-in in astrocytes shifts metabolism towards increased glucose usage and reduced fatty acid β-oxidation, leading to lipid accumulation[14, 16, 17]. Both microglia and astrocytes express enzymes for β-oxidation, with fatty acid metabolism influencing microglial phenotype and inflammation. Inhibition of β-oxidation in macrophages and microglia exacerbates inflammation while enhancing fatty acid oxidation reduces lipid-induced inflammation. Activation of mitochondrial function in microglia helps alleviate neuroinflammation and promotes amyloid-β clearance[18-20].

Neuroinflammation plays a critical role in AD, marked by elevated pro-inflammatory cytokines, reduced anti-inflammatory responses, and heightened glial cell reactivity. Lipids, particularly fatty acids, and their derivatives, have long been recognized for their immunomodulatory effects. Depending on the lipid class and the cell type, they can trigger either pro-inflammatory or anti-inflammatory responses[21-22]. In transgenic mice expressing a mutant APP, there was an increase in Aβ42 deposits in the brain along with elevated plasma cholesterol levels[79, 80]. A growing body of evidence, including the recent genome-wide association studies (GWAS) strongly supports the involvement of disrupted brain lipid metabolism in the pathogenesis of AD[81, 82]. Elevated levels of lysophospholipids and ceramides have been detected around Aβ plaques in human AD brain. Similarly, in *App*$^{NLG\text{-}F}$ knockin mice, an age dependent increase in

lysophospholipids and bis-phosphates (BMP) have been observed in the vicinity of Aβ plaques[83]. However, beyond these genetic factors, the role of lipid metabolism in AD pathology remains underexplored. Given the complexity of lipid metabolism and its regulation, understanding how lipid dysregulation contributes to AD could reveal new avenues for therapeutic intervention.

One of the key enzymes involved in lipid metabolism is Diacylglycerol O-acyltransferase 2 (Dgat2), which catalyzes the final step in triglyceride synthesis[23]. Interestingly, Dgat2 has been implicated in both lipid metabolism and the regulation of circadian rhythms, suggesting that its role extends beyond simple lipid storage and may influence the timing of metabolic processes[24-26]. Dgat2 expression in *Drosophila* and other animals is influenced by a variety of transcription factors, Ecdysone induced protein 75B (Eip75B), Ecdysone receptor (EcR), Nuclear factor of activated T-cells (Nfat) and Sterol regulatory element binding protein (Srebp), some of which are linked to lipid metabolism[90-93]. Even though the exact transcription factors that directly regulate Dgat2 are not as well-established as those that regulate other metabolic genes, such as those regulated by SREBP. Recent research indicates that Dgat2 inhibition reduces lipogenesis by blocking SREBP-1 cleavage and lowering Srebf1 gene expression in the liver[84, 85]. Recent studies have shown that Dgat2 is upregulated in AD models and human postmortem AD brains, suggesting a potential link between Dgat2 activity and AD pathology[27]. However, the precise mechanisms by which Dgat2 contributes to AD remain unclear, particularly in the context of neuropathology and lipid dysmetabolism associated with APP mutations.

Circadian rhythms, which regulate various physiological processes on a roughly 24-hour cycle, are disrupted in AD. These disruptions are linked to disturbances in sleep, metabolism, and cognition, which are hallmark features of the disease. Interestingly, circadian rhythms are known to influence lipid metabolism, and disruptions in circadian timing can lead to metabolic dysfunction, including altered lipid storage and degradation[28-30]. Time-restricted feeding (TRF), a behavioral intervention that restricts the timing of food intake to a specific window during the active period, has been shown to improve metabolic health and restore circadian rhythms. Importantly, TRF has been found to modulate lipid metabolism by regulating enzymes such as Dgat2[24, 25, 26]. This makes TRF a promising

therapeutic strategy for mitigating the metabolic disturbances seen in AD, and potentially halting or slowing disease progression[99, 100]. Our previous work has demonstrated that TRF, when combined with the downregulation of Dgat2, can improve lipid metabolism and muscle function in *Drosophila* melanogaster (commonly known as fruit fly), a widely used model organism for studying human diseases[24, 31]. Furthermore, we showed that the ApoE induces lipid accumulation in the brain, with ApoE4 uniquely causing this accumulation independently of Dgat2, unlike ApoE2 and ApoE3, which require Dgat2 for lipid buildup[24]. Additionally, TRF effectively prevents ApoE-induced lipid accumulation in the brain and modulates lipid metabolism genes[24]. These findings underscore the importance of lipid metabolism in AD and suggest that TRF could serve as a potential therapeutic approach to mitigate ApoE-related metabolic dysfunction. These findings suggest a strong connection between lipid metabolism and AD pathology[24].

Here, we use *Drosophila* and *mouse* models of AD to study the effect of APP and *Aβ42* with and without Dgat2 modulation (*Drosophila*) and with Dgat2 Inhibitor (Mouse) on lipid metabolism and AD-related phenotypes. Pan-neuronal, glial, and mushroom body-specific expression of *UAS-App^{NLG} UAS-Aβ42* to induce lipid dysmetabolism and neurodegeneration. For the mouse study, we use *App^{NLG-F}* knockin mice with elevated Aβ pathogenic levels due to the combined effects of three mutations associated with familial AD[94]. These mice develop amyloid plaques, neuroinflammation, synaptic loss, and cognitive deficits, providing a robust model to study the progression of AD. By modulating Dgat2, we examine the effects of Dgat2 inhibitor in AD mouse model, focusing on lipid metabolism, and neuroinflammation. Our innovative finding showed that in Drosophila models of *App^{NLG}* mutations and *Aβ42* led to progressive locomotor impairments, sleep disturbances, memory deficits, lipid accumulation, and neuroinflammation, with lipid dysregulation and inflammation. In this study, we observed that Dgat2 knockdown, led to improved inflammatory and metabolic gene expression and enhanced locomotor function, underscoring the potential benefits of modulating lipid metabolism through Dgat2 interventions. Additionally, Dgat2 modulation enhanced sleep quality and circadian rhythms, highlighting its role in AD progression. Using a mouse model of *App^{NLG-F}* we have shown that lipid accumulation and neuroinflammation occur. Dgat2 inhibition mitigated lipid dysmetabolism, decreased neuroinflammation responses,

and reduced expression of AD risk genes. These findings suggest that targeting Dgat2 may offer a potential therapeutic strategy for AD, emphasizing the conserved impact of lipid metabolism across species.

Material and Methods

Drosophila models

Flies were maintained on a standard regular diet: agar 11 g/L, active dry yeast 30 g/L, yellow cornmeal 55 g/L, molasses 72 mL/L, 10% nipagen 8 mL/L, and propionic acid 6 mL/L. Flies were housed at 25 °C, 50% humidity in a 12-h light/12-h dark (LD) cycle and changed to new food every 3-4 days[33-36]. We used the following driver's lines from Bloomington Drosophila Stock Center (BDSC) Elav(X)-Gal4 (BL#458) for panneuronal expression[95], GLaz-Gal4 (BL#8765) for glial expression[96] and OK107-Gal4 (BL#854) for mushroom bodies[97]. We used the following UAS lines UAS-APP^{NLG} (APP human APP carrying the familial Alzheimer's Swedish K670N, M671L, and Arctic E693G mutations, BL#33794) and UAS-Aβ42 (BL#33769). As previously described, we have also used UAS-hDgat2 (BL#84854), UAS-Dgat2 RNAi (BL#107788), and UAS-GFP (BL#5431)[24, 26, 78]. Moreover, we have also used the following RNAi stocks as potential transcriptions of Dgat2. UAS-Eip75B (BL#26717), EcR (BL#58286), UAS-Nfat (BL#51422), UAS-Vri (BL#25989), and UAS-Srebp (BL #25975). As recently reported flies that were Elav > DGAT2 or Elav > Dgat2 RNAi with a balancer[24], then crossing with UAS-APP^{NLG}, UAS-Aβ42 or control constructs, we used the *UAS-Gal4* system, permitting tissue-type expression or knockdown under specific region of the brain[98]. In addition to each UAS line driven under different drivers, the driver and UAS lines alone along RNAi control, GFP overexpression as controls as previously reported[24, 26, 78]. Briefly, the progeny of the above-mentioned crossed flies will be collected at eclosion, separated by sex, held at a density of 25 flies/vial, and maintained on the diet mentioned above. As indicated in the results section, experiments were performed on 3-week (early middle age) and 7-week-old (old age) male or female flies as previously reported[24, 26, 78].

Mice

All mouse breeding, procedures, and experiments were approved by the Institute Animal Care and Use Committee (IACUC) at the University of Alabama at Birmingham. Mice

were maintained in the Laboratory Animal Shared Resource with controlled air, light, and temperature conditions and fed ad libitum-free access to water. The *App*$^{NLG-F}$ mouse model is a genetically engineered strain used to study AD. It carries three familial AD-associated mutations in the APP gene: Swedish mutation *(NL),* which enhances total *aβ* production, Iberian mutation *(F),* increases the *Aβ42/ Aβ40 ratio and* Arctic mutation *(G),* which promotes Aβ aggregation by facilitating oligomerization and reducing proteolytic degradation[94]. The *App*$^{NLG-F}$ knockin mouse model with the following genotypes was generated as previously described[37]. *App*$^{NLG-F}$ and WT (controls), both were maintained in C57BL/6J background. The study was not pre-registered. Both WT and *App*$^{NLG-F}$ male mice with age of 4 months (n=3) and 15 months (n=3) were euthanized by cervical dislocation. Half brain for immunohistochemistry and half cortex for RNA.

Dgat2 Inhibitor

To investigate whether Dgat2 contributes to AD-related phenotypes, we used PF-06424439, a Dgat2 noncompetitive (MedChemExpress, CAS No#1469284-78-3), slowly reversible inhibitor with an IC50 of 14nM. We injected PF-06424439 intraperitoneally at 0, 10, and 30 mg/kg to 3 each male 12 months old *App*$^{NLG\text{-}F}$ mice daily for 5 consecutive days. The euthanizing method was the same as above.

Drosophila Olfactory aversion training to test memory

Flies were trained using olfactory aversive conditioning method as previously described[86, 87]. Approximately 30-40 group of flies were used for each genotype. Each genotype was exposed to two neutral odors (3-octanol and 4-methylcyclohexanol) prepared as a 1/10 dilution in mineral oil. A current of 100-V and 90-Hz was used as shock reinforcer. Memory conditioning was performed using T maze apparatus obtained from (CelExplorer Labs). The olfactory aversive conditioning consists of three phases: naïve, training and testing. During naïve phase, flies are exposed to both odors for 3 minutes and 30 seconds to determine their odor preference based on odor presented in each odor chamber. A single training round consist of exposing flies to odor paired with electrical shock for 2 minutes. Followed by 2 minutes of exposure to odor paired without shock. Depending on fly's naïve odor preference, electrical shocking will be paired with their preferred odor. After three training rounds, flies are given 10 minutes to recover. During testing phase flies are given 3 minutes and 30 seconds to choose between odor chambers. Once time has expired, T

maze chambers were sealed, and the number of flies in each chamber is scored. A performance index (PI) was calculated based on flies' avoidance of odor paired with electrical shock. To confirm these findings, we conducted a sensory acuity test based on avoidance index calculations, as previously described[68].

***Drosophila* locomotion assay**

To evaluate the panneuronal and glial-specific expression of APP mutation and the impact of Dgat2 KD and OE on locomotor capability, we have developed a new 3D-printer-based device to analyze locomotive performance, using machine learning methods (manuscript under preparation). Briefly, the device holds 12 vials and features a Raspberry Pi Camera aimed precisely at them, which is connected to a Raspberry Pi 4B and a monitor. A custom Python script developed in our lab is running on the Raspberry Pi, controlling both the camera and an attached motor system. Video was recorded after tapping the device and the Faster RCNN deep learning model was used to detect vial boundaries in the video. The flies' climbing behavior was recorded on video for later analysis. Followed by python analysis processes video frames for fly detection and detection across time for average climbing were plotted.

***Drosophila* sleep circadian activity**

Sleep-wake and circadian activity behavior was recorded using the Drosophila Activity Monitor (DAM, TriKinetics Inc MA, USA) system in a 12L: 12D cycle at 25°C[102]. We used 3 week and 7-week-old male and female progeny of Elav-Gal4 and GLaz-Gal4 with control lines of each of the four genes *(w^{1118}, GFP, App^{NLG}, Aβ42*). We have also used Dgat2 transcription factors KD genes, *Eip75b, EcR, Nfat, Vri, and Srebp).* Drosophila activity (or wake) is measured by infra-red beam crosses in the DAM system. Data was analyzed using Clock Lab and R Studio. Custom R scripts and methodology used with R Studio can be found at https://github.com/jameswalkerlab/Gill_et.al. One-way ANOVA with Dunnet's multiple comparisons test for DAM system data was performed using Graph Pad Prism. Drosophila sleep was defined by a period of at least 5 minutes of inactivity, demonstrated by zero beam breaks recorded. Average sleep per 24 hours (Zeitgeber Time (ZT) is a standardized way of measuring time within a circadian cycle, where ZT0-ZT24, ZT0 represents the beginning of the light phase and ZT12 marks the start of the dark phase), of each genotype, was calculated. Five days were used for analysis of 3-

week-old flies, and 3 days were used for 7-week-old fly experiments to overcome decreased viability in older flies. Sleep fragmentation was defined by the number of 1-minute wakes for 24 hours. Sleep bouts were quantified by counting the number of periods of sleep as defined above. Sleep bout length was quantified by measuring the length of each sleep bout. Data for daytime sleep is from ZT0 to ZT12, and nighttime sleep is from ZT12-ZT24.

Cytological analysis of *Drosophila* and Mouse brain samples

To investigate the impact of APP mutation and *Aβ42,* with and without Dgat2 modulation, on lipid and synapsin alternations will follow carried out as previously described[88, 24, 89]. Briefly, fly heads were excised under a dissecting microscope, then fixed in 4% paraformaldehyde (PFA) in phosphate-buffered saline (PBS) for 15 minutes at room temperature with mild agitation. The heads were washed three times for 10 minutes in 1× PBS, ensuring complete submersion, and stored at 4°C in PBS before cryosectioning. After the final wash, heads were transferred to a 10% sucrose in PBS solution, ensuring full submersion. They were placed into a labeled mold with approximately 50% Optimal Cutting Temperature (OCT) compound, which spread across all four corners of the mold. The samples were sectioned at 20µm using a Leica CM3050 S cryostat and mounted on glass slides (Fisher #15-188-48). After a 30-minute drying period, slides were washed three times for 5 minutes with 1× PBS to remove the dried OCT. The slides were then blocked with 3% BSA in TBS solution for 30 minutes and incubated overnight at 4°C or for 1 hour at room temperature with primary synapsin antibody (1:500, UI Developmental Studies Hybridoma Bank #3C11) in 1% BSA in TBS. After incubation, slides were washed three times for 5 minutes with PBS and incubated for 1 hour at room temperature with an AlexaFluor-594 anti-mouse fluorescent secondary antibody (1:1000, Thermo Fisher # A-11032). Finally, slides were washed three times for 5 minutes with 1× PBS and mounted with ProLong Diamond Antifade Mountant with DAPI (0.9µg/ml, Thermo Fisher # P36971). After overnight setting, multichannel fluorescence images were captured using an Olympus BX63F fluorescence microscope and analyzed with CellSens software at 10× magnification to view one section of the head per image. Fluorescence images were acquired using the Olympus BX-63 microscope, and lipid and synaptic alterations were quantified. Lipid accumulation was quantified using ImageJ88. Each multichannel image

was split into three channels: TRITC (red, measuring Nile Red lipids) and DAPI (blue, measuring cell nuclei). The DAPI channel was used to define regions of interest (ROIs), as it clearly distinguishes between anatomical sub-regions in the body. ROIs were manually drawn in ImageJ around the central brain, excluding the optic lobes. For each ROI, the mean fluorescent intensity of the TRITC channel was measured using ImageJ's measurement tool to quantify Nile Red staining intensity. Multiple sections were imaged for each fly, and the average fluorescent intensity across sections was calculated to determine the overall lipid accumulation value per fly.

Synapsin immunofluorescence intensity was quantified using FIJI software (ImageJ v1.53v). TRITC channel images were adjusted in batches to optimize the signal-to-noise ratio, and the mean fluorescent intensity for each image was measured within an ROI drawn around the brain. To account for background fluorescence, control samples were run in parallel without primary antibody. The background fluorescence from the brain was measured and subtracted from the fluorescence value for each image. At least two sections per fly were imaged, and the mean fluorescence per fly was calculated and reported.

Mice brain staining, imaging, and image quantification

One brain hemisphere was placed in 4% paraformaldehyde overnight at 4ºC followed by sucrose incubation until saturated. The brain sample was frozen in OCT blocks and stored at -80ºC. 10µm tissue was cryosectioned and ready for staining. Nile red (Sigma: N3013) and LipidSpot™ 488 (Biotium NC1669425) were for Lipid Droplet Staining following the company's instructions. Gfap (Dako: Z0334, 1:20,000) or Iba1/AIF-1 (Cell Signaling Technology 17198S: 1:100) were paired with secondary Alexa fluor 488 (Invitrogen cat# A11008, 1:1,000). Hoechst (Fisher PI62249) was used as a nuclear stain. Images were acquired using the Keyence BZ-X810 microscope and ImageJ was used for image analysis.

Real-time quantitative PCR in *Drosophila* and mouse brain samples

As previously reported[24], the heads of 3-week-old and 7-week-old flies were isolated and rapidly frozen. RNA extraction was performed using the Zymo Research Quick-RNA Microprep Kit (catalog R1051, Zymo Research, Irvine, CA, USA), which included on-column DNase I digestion. Quantitative PCR was conducted using the Sso Advanced

Universal SYBR Green supermix from Bio-Rad, employing the BIO-RAD CFX Opus Real-Time PCR System. Expression levels were standardized using the 60s ribosomal protein (Rpl11) as a reference three biological replicates were used with 8-10 flies each. Primers for qPCR are listed below:

Upd1-F: CAGCGCACGTGAAATAGCAT; Upd1-R: CGAGTCCTGAGGTAAGGGGA;
Upd2-F: AGCGTCGTGATGCCATTCA; Upd2-R: GCGATACGGATTGACATCGAA;
Upd3-F: ATCCCCTGAAGCACCTACAGA; Upd3-R: CAGTCCAGATGCGTACTGCTG;
Dome-F: CTCACGTCTCGACTGGGAAC; Dome-R: AGAATGGTGCTTGTCAGGCA;
Hop-F: CACCACCAACACCAATTC; Hop-R: GGAACGTCGTTTGGCCTTCT;
Stat92e-F: CCTCGGTATGGTCACACCC; Stat92e-R: TGCCAAACTCATTGAGGGACT;
Eiger-F: GATGGTCTGGATTCCATTGC; Eiger-R: TAGTCTGCGCCAACATCATC;
Imd-F: TCAGCGACCCAAACTACAATTC; Imd-R: TTGTCTGGACGTTACTGAGAGT;
Reaper-F: TGGCATTCTACATACCCGATCA;
Reaper-R: CCAGGAATCTCCACTGTGACT;
Hid-F: CACCGACCAAGTGCTATACG; Hid-R: GGCGGATACTGGAAGATTTGC;
Rpl11-F: CGATCTGGGCATCAAGTACGA; Rpl11-R: TTGCGCTTCCTGTGGTTCAC;
Desat2-F: GTCGGCTACCCCTAGTCTGG; Desat2-F: TCGCCCTTGTGAATATGGAGT;
Amph-F: TCAAGTCCTCATTCCGCTCAA; Amph-R: CGGTTGCGCTTCTCTACTTTT;
Abca3-F: GCTCCTCGTTCTAGTCCGC; Abca3-R: TTGCAGCAGATTGAGGTCTGT;
Eph-F: TTGGCACATGCAGATCAGGTT; Eph-R: TGGTGTTTGGGCTTGAGGTC;
Ank-F: AGCTGCAATGCAAACGGTCT; Ank-R: CCCCTTCTTAGCAACTCGCA;
Rho5-F: GGAAACGGAATGGCGGCTAA; Rho5-R: ATTGCGGAGTTGACTGCGATT;
Nlaz-F: ACGCCAACTACAGTCTCATAGA; Nlaz-R: CGAGGGTTGTCCGGTGAATC;
Eip75b-F: ATGCAACAGAGCACCCAGAAT;
Eip75b-R: CATGGAGTAGGAGGGGCAATC;
Nfat-F: AAAGACAGCCGGGTAAGGGAT; Nfat-R: CAGGAACCATTTTGCCAGGAC;
EcR-F: GTCCCGGAGAACCAATGTG; EcR-R: GGCGAAGTGGTCATTTTGTCC;
Srebp-F: ACCAACAGCCACCATACATCA; Srebp-R: AGACAAAGCTACTGCCCAGAG;
Dgat2-F: ATCCGTTGTGGATGGCAATG;
Dgat2-R: GGGAAAGTAATCACGATAGTGGC;
Eda-F: AGTGCTCAATGACTGGTCTCG; Eda-R: CGCTGCGGGGATGTAGTTTA;

Stat5b-F: CGATGCCCTTCACCAGATG; Stat5b-R: AGCTGGGTGGCCTTAATGTTC;
Ptprq-F: ATTTCTGCCACAACCTACAGC;
Ptprq-R: GGAGGGGTATTCCATGAAAGGAG;
Jak2-F: TTGTGGTATTACGCCTGTGTATC; Jak2-R: ATGCCTGGTTGACTCGTCTAT;
Ripk1-F: AGAAGAAGGGAACTATTCGCTGG;
Ripk1-R: CATCTATCTGGGTCTTTAGCACG;
Scd1-F: TTCTTGCGATACACTCTGGTGC; Scd1-R: CGGGATTGAATGTTCTTGTCGT;
Amph-F: TCAAGTCCTCATTCCGCTCAA; Amph-R: CGGTTGCGCTTCTCTACTTTT;
Abca3-F: GCTCCTCGTTCTAGTCCGC; Abca3-R: TTGCAGCAGATTGAGGTCTGT;
Eph-F: TTGGCACATGCAGATCAGGTT; Eph-R: TGGTGTTTGGGCTTGAGGTC;
Ank-F: AGCTGCAATGCAAACGGTCT; Ank-R: CCCCTTCTTAGCAACTCGCA;
Rho5-F: GGAAACGGAATGGCGGCTAA; Rho5-R: ATTGCGGAGTTGACTGCGATT;
Nlaz-F: ACGCCAACTACAGTCTCATAGA; Nlaz-R: CGAGGGTTGTCCGGTGAATC;
Nfat-F: AAAGACAGCCGGGTAAGGGAT; Nfat-R: CAGGAACCATTTTGCCAGGAC;
EcR-F: GTCCCGGAGAACCAATGTG; EcR-R: GGCGAAGTGGTCATTTTGTCC;
Srebp-F: ACCAACAGCCACCATACATCA; Srebp-R: AGACAAAGCTACTGCCCAGAG;
Dgat2-F: ATCCGTTGTGGATGGCAATG;
Dgat2-R: GGGAAAGTAATCACGATAGTGGC;
Eda-F: AGTGCTCAATGACTGGTCTCG; Eda-R: CGCTGCGGGGATGTAGTTTA;
Stat5b-F: CGATGCCCTTCACCAGATG; Stat5b-R: AGCTGGGTGGCCTTAATGTTC;
Ptprq-F: ATTTCTGCCACAACCTACAGC;
Ptprq-R: GGAGGGGTATTCCATGAAAGGAG;
Jak2-F: TTGTGGTATTACGCCTGTGTATC; Jak2-R: ATGCCTGGTTGACTCGTCTAT;
Ripk1-F: AGAAGAAGGGAACTATTCGCTGG;
Ripk1-R: CATCTATCTGGGTCTTTAGCACG;
Scd1-F: TTCTTGCGATACACTCTGGTGC; Scd1-R: CGGGATTGAATGTTCTTGTCGT;
Results are presented as 2−ΔΔCt values normalized to the expression of Rpl11 and. All reactions were performed in triplicate.

Mouse RNA extraction was performed by using RNeasy Plus Mini Kit (Qiagen, Cat#: 74134) from isolated mouse cortex samples. cDNA synthesis was performed using a

High-Capacity cDNA Reverse Transcription Kit (Thermo Fisher Scientific, Cat#: 4368814). Primers for mouse qPCR are listed below:

Bin1-F: TTCGGACCTATCTGGCTTCTG; Bin1-R: CCTCCTGAAGACACTCACTCA;
Abca7-F: AATTACACCTATCGACGGAGACA; Abca7-R: TGACGGACAGCCACTAGGA;
Cass4-F: CCAGGGCACTCTACGACAAC; Cass4-R: GCACATTTTGTTCCACGATGG;
Eph1-F: AGGAAGTCACTCTAATGGACACA; Eph1-R: CCTCACTCCACCCAGTCTCT;
Ank1-F: GGAGCGTCACCCAATGTCTC; Ank1-R: GGCCACTTCTGTATGCCCTG;
Rhbdf2-F: GCCCACACCGTATCTGTTCTG;
Rhbdf2-R: GATGCCAGTTTTGTCGCTTGC;
Apoe-F: GACCCAGCAAATACGCCTG; Apoe-R: CATGTCTTCCACTATTGGCTCG;
Nr1d1-F: ACTTCCCACCATCACCTACTG; Nr1d1-R: GGGGAGCTATCATCACTGAGA;
Nfat5-F: GAGGGGTGTGGATTGGAATCT;
Nfat5-R: CTGGTGCTCATGTTACTGAAGTT;
Nr1h2-F: GCCTGGGAATGGTTCTCCTC; Nr1h2-R: AGATGACCACGATGTAGGCAG;
Srebf1-F: TGACCCGGCTATTCCGTGA; Srebf1-R: CTGGGCTGAGCAATACAGTTC;
Picalm-F: CTGACGGACCGAATCACCG; Picalm-R: GTGGCCTTGCATACTGTCTTAG;
Dgat2-F: TTCCTGGCATAAGGCCCTATT; Dgat2-R: CCTCCAGACATCAGGTACTCG;

Results are presented as $2^{-\Delta\Delta Ct}$ values normalized to the expression of β-actin.

Statistical analysis

Significance sleep-circadian activity and climbing ability were determined using one-way ANOVA or two-way ANOVA with post hoc Sidak's method for multiple comparisons or two-sided unpaired t-tests. Lipid droplet size and density differences and synaptic loss were performed by one-way ANOVA with post hoc Sidak's method or two-sided unpaired t-tests. For sleep activity analysis, differences between samples were determined using two-way ANOVA with post hoc Sidak's method. PCR analyses were made using two-way ANOVA with post hoc Sidak's method in both *Drosophila* and mouse samples. Bar graphs show mean ± SEM. All statistical analyses were performed with Graph Pad Prism 10.

Results

A brief outline of our study is shown in **Fig.1a**, to reveal the involvement of beta amyloid in the progression of AD across the species using *Drosophila* and mouse models. As indicated in the method section, using *Drosophila* models, we have tested the impact of *UAS-App*^{NLG} *UAS-Aβ42*) upon their expression in panneuronal (Elav), glial (GLaz) and mushroom body (Ok-107) drivers. The outline also demonstrated the specific assays as well as the involvement of *Dgat2 knock-down (KD)* and over-expression (OE) of human Dagt2 (hDgat2) in modulating AD phenotype in a *Drosophila* model. As shown in Fig. 1a geotaxis assays were performed to assess locomotor performance and sleep-circadian activity were conducted using the DAM system upon expression of APP mutation and revealing the impact of Dgat2 modulation. As previously reported brain lipid accumulation and olfactory aversion training was performed to test memory upon expression of APP mutants with or without Dgat2 modulations. Using qPCR, we also performed gene expression analyses of key genes involved in, lipid metabolism, neuro-inflammation, and other AD risk genes upon expression of APP mutation and to impact of Dgat2 modulation. All experiments were done with their respective controls (W^{1118} and GFP) at two different ages **(Fig. 1a).**

As demonstrate in Fig.1a, we used the *App*$^{NLG-F}$ mouse model of AD, along with their respective control mice. In a mouse AD model, immunofluorescence was used to examine lipid accumulation and glial fibrillary acidic protein (GFAP) level representing glial activation. We also performed gene expression analyses using qPCR for the genes associated with lipid metabolism, neuroinflammation, and AD risk genes in the *App*$^{NLG-F}$ mouse model. In addition, we used Dgat2 inhibitor to examine the impact of these inhibitor on lipid accumulation and neuroinflammation and the expression of AD risk genes **(Fig. 1a).**

Panneuronal, glial or mushroom-body specific expression of A*pp*^{NLG} *and Aβ42* led to compromised locomotor and/or cognitive performance

As shown in **Fig.1b**, we observed distinct differences in compromised locomotor performance upon expression of *App*^{NLG} and A*β42,* which was prominent with the expression of Aβ42, and modestly so of *App*^{NLG} in females, compared to age-matched control in 3-week-old flies **(Fig.1b)** Similar trends were observed in male flies with Elav-

Aβ42, whereas male flies expressing *App^{NLG}* construct showed no significant changes in the climbing ability regardless of the driver used**.** These results suggest that the geotaxis phenotype is driver-specific and impacts locomotor performances prominently in females than male flies, whether through panneuronal or glial specific expression **(Fig.1b).** Drosophila can learn to associate odors with negative or positive reinforcers. After training, flies can learn to avoid or approach the odor paired with reinforcer. To investigate whether cognitive performance was comprised in *App^{NLG}* and *Aβ42* using Elav, GLaz, and OK107 drivers **(Fig.1c-e).** We subjected wild type, *App^{NLG}* and *Aβ42* flies to olfactory aversive conditioning. Knockdown expression in 3-week-old female flies driven with Elav and GLaz resulted in significant impaired cognitive performance **(Fig. 1c, d, left panels).** Next, we tested the effect of expressing AD-linked genes in the mushroom body using the OK-107 driver. Remarkably, flies with expression of these genes in the mushroom bodies, both *App^{NLG} and Aβ42* models, showed a significant impairment in olfactory aversion training **(Fig. 1e, left panel).**

In addition, we also employed two olfactory aversion analyses, which evaluates sensory acuity through both odor acuity (measured by the odor avoidance index) and shock acuity (measured by electric shock avoidance index) **(Fig 1 d-e, middle and right panels respectively).** Both approaches resulted in the similar conclusion. These results suggest that the expression of AD-linked genes in the mushroom bodies has a profound effect on memory, then compared to pan-neuronal and glial expression region, which is consistent with the critical role of these brain regions in olfactory learning. This suggests that different brain regions are involved in cognitive dysfunction in these models, providing further insight into the mechanisms underlying AD-related memory impairment.

Compromised circadian activity in flies with panneuronal and glial-specific expression of *Aβ42 and in* aged glial-specific expression of *App^{NLG}*

A variety of sleep/ circadian parameters including day, night, and total sleep duration, circadian activity, and sleep quality parameters in 3 and 7-week-old male flies with the pan-neuronal and glial specific expression of *App^{NLG}* and *Aβ42 and controls* was analyzed ***(Fig. 2 and Extended Data Fig. 1a-c, Fig. 2a-c, Fig. 3a-f)*.** We performed these assessments, focusing on sleep duration, sleep profile, sleep fragmentation, bout length,

and bout number. These data were compared to control flies to evaluate the impact of the AD mutations on sleep behavior ***(Fig. 2 and Extended Data Fig. 1a-c, Fig. 2a-c, Fig. 3a-f)*.** As shown in **Fig. 2a,** neuronal-specific expression of *Aβ42* exhibited a significant increase in overall sleep time compared to controls in 3wk old flies. This increase was primarily observed during the night, as nighttime sleep duration was notably longer **(Fig. 2a),** as sleep profile showing sleep minutes/ hours for 24 hours **(Fig. 2b)**. Interestingly, this increase in sleep time was accompanied by a rise in sleep fragmentation, which was most pronounced during the nighttime **(Fig. 2c),** upon neuronal-specific expression of *Aβ42.* This trend was also evident upon expression of App^{NLG} **(Fig. 2a-c),** but statistically not significant. These findings suggest that while the pan-neuronal-specific expression of *Aβ42* led to more sleep, sleep quality was compromised as indicated by higher sleep fragmentation **(Fig. 2a-c)**

As shown in **Fig. 2d and Extended Data Fig. 2a-c,** flies with glial-specific expression App^{NLG} and *Aβ42* genes exhibited significantly increased sleep in *Aβ42,* which was primarily due to extended sleep during the nighttime, as sleep profile showing sleep minutes/ hours for 24 hours **(Fig. 2e).** This increase in sleep was associated with higher sleep fragmentation during the nighttime in App^{NLG} and total sleep fragmentation in both App^{NLG} and *Aβ42* **(Fig. 2f),** suggesting that while the total sleep duration increased, the quality of sleep was negatively impacted. The elevated sleep fragmentation further emphasizes the adverse effects of App^{NLG} and *Aβ42* on sleep.

Additionally, we observed a significant decrease in the total number of sleep bouts, particularly during the night, upon panneuronal expression of *Aβ42* indicating that the flies experienced fewer, longer sleep periods in 3-week-old male flies **(Extended Data Fig. 1b-c)**. On the other hand, in the GLaz-driven App^{NLG} and *Aβ42*, there was an increase in the number of sleep bouts during the day, along with longer day bout lengths, suggesting a different pattern of sleep fragmentation in glial-specific AD models **(Extended Data Fig. 2a-c).** Like 3-week-old flies observed similar trends in sleep activity parameters in 7-week-old male flies, showing that the sleep disruptions caused by Elav and GLaz-driven AD genes persisted and became progressive with age **(Extended Data Fig. 3a-f).** This suggests that sleep disturbances in App^{NLG} and A*β42* flies are not merely a transient phenomenon but rather a lasting feature of the disease model.

Panneuronal and glial specific expression of *App^{NLG}* and *Aβ42* led to increased lipid accumulation and reduced synapsin levels

Our results revealed a significant increase in lipid accumulation, as indicated by green positive cells in both the *App^{NLG} and Aβ42* flies, compared to their respective control groups at 3 week **(Fig. 3a-f).** Notably, panneuronal-driven *App^{NLG} and Aβ42* flies exhibited more prominent lipid accumulation than glial drivers. This suggests that lipid dysregulation is a prominent feature of *App^{NLG} and Aβ42* models, potentially contributing to lipid dysregulation in these models. Additionally, synapsin expression was markedly reduced in both *App^{NLG} and Aβ42* flies. Synapsin staining intensity was significantly lower in these flies compared to controls, indicating impaired synaptic function **(Fig. 3d, f).** This reduction was observed in both panneuronal and glial-driven *App^{NLG} and Aβ42* flies. At 7 week, lipid accumulation remained elevated in both the *App^{NLG} and Aβ42* flies in both panneuronal and glial drivers, while synapsin level showed no change with panneuronal driven flies but were reduced in glial driven *App^{NLG}* model, suggesting a stabilization or compensatory adaptation in synaptic function (**Extended Data Fig.4a-f**). This comparison between 3 and 7 weeks indicates an early phase of synaptic damage followed by a potential plateau in synaptic decline, with persistent lipid and amyloid changes indicating ongoing pathophysiological processes. These findings suggest the *App^{NLG}* model may better replicate the synaptic dysfunction seen in AD, potentially leading to greater cognitive and sleep disturbances. Together, these results provide strong evidence that lipid dysregulation and synapsin impairment are linked in AD progression.

***App^{NLG-F}* mice exhibit age dependent increase of lipid accumulation and glial activation**

Next, we performed immunostaining in the cortex (Ctx) region of the *App^{NLG-F}* mice to assess the level of lipid spot staining and GFAP immunoreactivity respectively with age (young and old mice). In *App^{NLG-F}* mice, we observed a notable increase in lipid spot-

positive cells with age. Specifically, a significant accumulation of lipids was evident in the Ctx of 15-month-old *App*$^{NLG-F}$ mice **(Fig.3g, i)**
Additionally, a higher abundance of GFAP was detected in the Ctx of these 15-month-old wild-type (WT) controls **(Fig. 3h, j).** This increase in GFAP expression was statistically significant in the cortex of 15-month-old *App*$^{NLG-F}$ mice relative to the age-matched WT counterparts.

We also examined the level of Nile red and Dgat2 staining in the Ctx (**Extended Data Fig.4g-j**), and found significant increase of Nile red staining and no change in Dgat2 stain in old *App*$^{NLG-F}$ mice. DGAT2 staining in the hippocampal CA1 region and cerebellum (CB) (**Extended Data Fig.5a-d**) have found increased Dgat2 aggregates in old *App*$^{NLG-F}$ mice. In addition, we assessed the expression of Adrp, a protein that binds lipid droplets in the cytoplasm, in the cortex and hippocampal CA1 regions (**Extended Data Fig.6a-d**). Interestingly, no significant changes in Adrp levels were observed in either region. Moreover, we examined GFAP and Iba1 expression in the CA1 regions (**Extended Data Fig.7a-d**). We found that the number of GFAP-positive cells was significantly higher in the 15-month-old *App*$^{NLG-F}$ mice compared to all other experimental groups. Additionally, Iba1-positive cells were also significantly increased in both young and old *App*$^{NLG-F}$ mice compared to age-matched control. Notably, aging did not seem to affect Iba1 expression in WT mice. However, a dramatic increase in Iba1 expression was observed in the 15-month-old *App*$^{NLG-F}$ mice when compared to the younger *App*$^{NLG-F}$ mice. These findings suggest that aging in *App*$^{NLG-F}$ mice is associated with increased lipid accumulation, enhanced astrocytic activation, and microglial changes in the brain, pointing to potential age-related pathological features such as neuroinflammation in these models of AD.

Age-dependent increase in neuroinflammation and AD risk gene expression in the *App*$^{NLG-F}$ mouse model

In the *App*$^{NLG-F}$ mouse model, we observed a significant age-dependent increase in Iba1, which is a marker of microglia activation **(Fig. 4a, b and Extended Data Fig.7a-d).** In the *App*$^{NLG-F}$ mouse model, this age-dependent rise in Iba1 suggests that microglia become more activated over time, possibly due to the accumulation of amyloid plaques in the

brain. While microglia initially respond to plaques and other damage in the brain by becoming activated to clear harmful debris, chronic activation can lead to neuroinflammation, as the microglia may become less efficient with age. This persistent activation can exacerbate neuronal damage and is thought to contribute to the progression of neurodegenerative diseases like Alzheimer's. This suggests a progressive activation of microglia with age, a hallmark of neuroinflammation. To further explore this, we examined the expression of key inflammatory genes, including protein tyrosine phosphatase receptor type Q (Ptprq), which also showed marked upregulation with age **(Fig. 4c)**, supporting the idea of chronic, age-related inflammation. Interestingly, other inflammatory markers, such as Janus kinase2 (Jak2), ectodysplasin (Eda), and signal transducer and activator of transcription 5B (Stat5b) did not show significant change in the expression, suggesting a more selective inflammatory response in this model. These findings point to the possibility that neuroinflammation plays a crucial role in neurodegeneration within the $App^{NLG\text{-}F}$ mouse model. In addition to inflammation, we assessed the expression of metabolic genes. Notably, Srebf1 expression was significantly increased with age, while no significant changes were observed in other metabolic genes, such as stearoyl-CoA desaturase (Scd) and Dgat2, indicating a possible alteration in lipid metabolism during aging **(Fig. 4d)**.

Further investigation of AD risk genes revealed an age-dependent increase in the expression of Bridging integrator 1 (Bin1) and ATP binding cassette subfamily A member 7 (Abca7), both of which are involved in amyloid processing and lipid transport. This upregulation suggests a potential link to increased amyloid burden or alterations in lipid metabolism, both of which are key features of Alzheimer’s pathology. Additionally, we observed elevated expression of rhomboid family-like 2 (Rhbdf2) and Apoe genes that are also associated with neuroinflammation and lipid homeostasis **(Fig. 4e)**. Taken together, the increased expression of Iba1, Ptprq, and several AD risk genes with age highlights the progressive activation of neuroinflammatory pathways and suggests that lipid metabolism and inflammatory responses may be central contributors to the neurodegenerative processes in the $App^{NLG\text{-}F}$ mouse model. This growing evidence reinforces the idea that neuroinflammation and the dysregulation of Alzheimer’s-related pathways progressively exacerbate pathology as the mice age.

App^{NLG} and *Aβ42*-linked locomotor and cognitive dysfunction was improved with Dgat2 KD and further aggravates Dgat2 OE

We assessed Geotaxis, and cognitive function, in 3 week old flies to investigate the effects of App^{NLG} and *Aβ42* in relation to the panneuronal expression of *Dgat2KD* and OE. First, we performed a geotaxis assay to evaluate locomotor performance and determine how these genetic manipulations influenced fly movement. At 3 weeks of age, we observed distinct differences in locomotor performance between flies expressing the App^{NLG} gene and their respective controls **(Fig.5a).** Both male and female flies showed varying responses to the *Dgat2 KD* and OE constructs. Specifically, male flies expressing under the control of the panneuronal driver in the *Dgat2 KD* condition exhibited significantly improved climbing ability, when they expressed App^{NLG} *or Aβ42)* **(Fig.5a).** Female flies showed similar trends, though the results were less statistically significant. In contrast, flies expressing the Dgat2 OE with the *Aβ42 and* App^{NLG} constructs did not exhibit any significant improvement in climbing ability compared to controls **(Fig.5a).** These results suggest that *Dgat2 KD* may have a protective effect, enhancing locomotor ability, while Dgat2 OE has the opposite effect, potentially worsening locomotor performance **(Fig. 5a).**

We next, evaluated if cognitive performance was altered in *Dgat KD* and OE. We used 3-week-old male flies expressing *GFP, Aβ42, and* App^{NLG} showed a rescue of memory impairment when Dgat2 was KD. However, memory impairment was not rescued in flies expressing Dgat2 OE **(Fig. 5b, c, left panel).** To calculate flies odor avoidance, we conducted performance index previously described in figure 1 (Meschi et al., 2024). The results from this method were consistent with our primary findings, further supporting the idea that the effects of Dgat2 manipulation on both locomotion and cognition are interconnected (**Fig. 5b, c, right panel).** In conclusion, these findings suggest that Dgat2 knockdown may confer a protective effect, improving both locomotor and cognitive functions, while Dgat2 overexpression appears to exacerbate deficits.

Dgat2 KD leads to the restoration of sleep activity and reduced sleep fragmentation linked with the expression of App^{NLG} and *Aβ42*

Next, we assessed the sleep activity in Elav-driven Dgat2 KD and OE flies at both 3 and 7 weeks of age to explore the potential links between sleep, cognitive function, and memory performance which were observed in earlier tests in *App*^{NLG} and *Aβ42*. At 3 weeks of age, both Dgat2 KD and Dgat2 OE flies expressing *Aβ42* exhibited a more prominent increase in total sleep, including daytime and nighttime sleep compared to *App*^{NLG}. In addition, both groups (Dgat2 KD and OE) showed reduced sleep fragmentation, indicating a more continuous sleep pattern. Importantly, there were no significant differences between the sleep patterns of Dgat2 KD and Dgat2 OE flies at 3-week age **(Fig. 5d, e).** These findings suggest that, despite the varying effects on cognition and locomotion, Dgat2 manipulation at 3 weeks does not drastically disrupt sleep. Instead, both groups exhibited increased total sleep and reduced fragmentation, implying that the overall sleep architecture is relatively similar between the two conditions. To further investigate, we examined additional sleep parameters. In the *App*^{NLG} and *Aβ42* models, we observed changes in sleep activity, such as decreased sleep bouts and increased bout length, particularly in *App*^{NLG} *and Aβ42* flies with Elav-driven Dgat2 KD. A similar trends were observed in the Dgat2 OE group, with reduced sleep activity and increased bout number and bout length, reinforcing the notion that Dgat2 manipulation alters sleep patterns in *App*^{NLG} *and Aβ42* models **(Extended Data Fig. 9, 10a-c).** However, when we assessed sleep patterns in 7-week-old flies, we found that the sleep behavior in *App*^{NLG} and *Aβ42* models with *Dgat2 KD* and Dgat2 OE was largely unchanged compared to the younger 3-week-old flies **(Extended Data Fig. 11a-d).** In other words, the sleep patterns of older flies were not significantly affected by Dgat2 manipulation, suggesting that the impact of *Dgat2 KD* or OE on sleep may be age dependent.

Dgat2 knockdown suppressed lipid metabolism, restored synaptic loss, and reduced inflammation associated with *App*^{NLG} *and Aβ42*

We first assessed immunostaining in Elav-driven *Dgat2 KD* flies expressing *App*^{NLG} *and Aβ42* to explore potential changes in lipid metabolism and synaptic function at 3 week. At this early age, we observed that lipid accumulation, typically elevated in *App*^{NLG} *and Aβ42* models, was significantly reduced in the presence of *Dgat2 KD.* This suggests that *Dgat2*

KD mitigates abnormal lipid buildup associated with AD models. Interestingly, synapsin levels were notably elevated in these flies **(Fig. 6a-c).** The increase in synapsin suggests that synaptic function might be improved, or compensatory mechanisms could be activated in response to the altered lipid metabolism in *App^{NLG} and Aβ42* models. **When** we assessed lipid accumulation at 7 weeks, we found that lipid levels remained reduced in the presence of *Dgat2 KD,* suggesting sustained mitigation of lipid dysregulation. However, synapsin levels were unaffected at 7 weeks **(Extended Data Fig. 12a-c),** indicating that despite the continued reduction in lipid accumulation, synaptic function may have reached a plateau or stabilization. This comparison between 3 and 7 weeks suggests that *Dgat2 KD* continues to modulate lipid metabolism, but its effect on synaptic function may be more complex or time-dependent, with a potential long-term stabilization in synaptic markers **(Extended Data Fig. 12a-c).**

To further validate these findings, we examined the expression of neuroinflammatory markers. The levels of primary inflammatory cytokines, including unpaired1 (Upd1) and, unpaired3 (Upd3), were significantly reduced Dgat2 KD flies, both without and with expressing *App^{NLG} and Aβ42*. This reduction indicates a decrease in neuroinflammation, suggesting that Dgat2 KD may help alleviate inflammation in these models. However, when we examined the expression of domeless (Dome) and Hopscotch (Hop) receptors, a key component of the JAK/STAT pathway, we observed an increase in their expression, both without and with expressing *App^{NLG} and Aβ42* **(Fig. 6d).** This suggests that the reduction in neuroinflammation due to Dgat2 KD oppositely modulates the JAK/STAT pathway.

Next, we assessed the expression of key metabolic markers Abca and Dgat2. Result shows that Abca expression was increased in the presence of Dgat2 KD in *App^{NLG} and Aβ42* models of *Drosophila* **(Fig. 6e).** This increase in Abca could reflect a compensatory response to the altered lipid metabolism and the Dgat2 KD, potentially helping to maintain lipid homeostasis in the context of neurodegenerative disease models.

Dgat2 inhibition led to microglial activation which further leads to reduced Dgat2 transcription factors and AD risk genes in a mouse model of *App^{NLG-F}*

For additional validation, we used mouse brain samples and performed lipid spot staining and GFAP immunofluorescence in the presence of a Dgat2 inhibitor **(Fig. 6f).** In this experiment, we found that lipid spots significantly increased, contrary to our finding in the flies that the Dgat2 KD decreased lipid accumulation **(Fig. 6g).** The contrasting results may arise from species-specific differences in lipid metabolism and compensatory mechanisms, with Drosophila showing reduced lipid accumulation due to direct Dgat2 KD, while mice exhibit increased lipid spots possibly as a compensatory response to disrupted lipid homeostasis**.** GFAP expression remained unchanged in the presence of Dgat2 inhibitor **(Fig. 6h).** This suggests that Dgat2 inhibition at this dose and frequency does not affect astrocyte activation in *App*$^{NLG\text{-}F}$ mouse model. In the mouse brain cortical region, Nile Red staining and Adrp expression did not show significant changes **(Extended Data Fig. 12d-i),** indicating that baseline lipid accumulation or storage was unaffected under normal conditions. Nile Red staining revealed an increased trend of number of lipid spots, suggesting enhanced lipid accumulation. This increase in lipid spots was accompanied by an upregulation of Dgat2 expression, as indicated by stronger Dgat2 staining, which points to a compensatory mechanism in response to the inhibition. The upregulation of Dgat2 protein likely contributes to the observed increase in lipid droplets, as the brain attempts to maintain lipid homeostasis despite the inhibition of Dgat2.

In contrast, we observed a significant increase in Ptprq expression. On the other hand, the expression of key AD risk genes, such as Abca7, Cass4 and Rhbdf2, was notably decreased in the presence of Dgat2 inhibitor, suggesting a potential downregulation of processes involved in amyloid processing and lipid transport **(Fig. 6i).** Additionally, Iba1 expression, a marker of microglial activation, was also unaffected **(Extended Data Fig. 13a, b),** indicating no direct modulation of microglial activation by Dgat2 inhibition. Additionally other inflammatory markers such as Jak2, Ripk1 and additional AD risk genes, like Bin1, Apoe, Eph, and Ank1 remained unaffected, highlighting a selective modulation of specific inflammatory pathways by Dgat2 inhibition **(Extended Data Fig. 13c-e).**

The expression of potential Dgat2 transcription factors (TFs) expression was elevated in *App^{NLG} and Aβ42* models and their panneuronal specific KD led to altered sleep circadian activity

To address whether Dgat2 transcription factors play a role in regulating sleep and circadian activity, we first assessed the relative gene expression levels using qPCR to determine the expression of potential transcriptional regulators of Dgat2. Our results revealed that Eip75b, EcR, Nfat, and Srebp all of which are involved in lipid metabolism and cellular stress responses, were significantly upregulated in Elav-driven *App^{NLG}, and Elav-Aβ42* model **(Fig. 7a).** Because their potential in Dgat2 regulation[84,85,90-93], these transcription factors might play a pivotal role in regulating Dgat2 expression and could contribute to the pathophysiology of AD by influencing lipid metabolism, synaptic function, and neuroinflammatory responses. In our next experiment, we examined changes in sleep activity following the KD of specific TFs that regulate Dgat2 expression. Previous result **(Fig5 d, e)** shows *Dgat2 KD* leads to the restoration of sleep activity and reduced sleep fragmentation in the *App^{NLG} and Aβ42* flies' models. Now, with *Dgat2* transcription factors *KD,* we found that, total sleep was significantly decreased in both *EcR* and *Srebp KD* flies, indicating that these transcription factors are involved in maintaining overall sleep duration. In contrast, day sleep was notably reduced in *Eip75b KD flies*, as well as in *EcR* and *Srebp* KD flies, indicating that these TFs are involved in regulating daytime sleep. Furthermore, we observed that sleep activity was significantly increased in the KD groups, which supports the overall findings **(Extended Data Fig. 14a)**. We also assessed sleep fragmentation and observed significant changes in this aspect of sleep regulation. Both total and night sleep fragmentation was significantly reduced in the *Nfat KD* group, indicating that Nfat plays a crucial role in maintaining sleep stability and continuity. On the other hand, day sleep TFs may be involved in processes that regulate daytime sleep fragmentation **(Fig.7b).** Additionally, *Nfat KD* displayed decreased bout numbers and increased bout length, further supporting the idea that Nfat contributes to the stability of sleep **(Extended Data Fig. 14b, c)**. These findings suggest that different TFs involved in Dgat2 regulation contribute to various aspects of sleep, such as overall duration, timing (day vs. night), and sleep fragmentation **(Fig.7b).**

Knock-down of Dgat2 transcription factors leads to reduced lipid accumulation and reduced expression of AD linked genes

To further investigate the impact of TF KD on lipid metabolism and synaptic regulation, we assessed lipid and synapsin dysregulation in the Dgat2 TFs KD groups. Our results showed a significant reduction in lipid accumulation in the *Srebp KD, Eip75b KD, and Nfat KD* groups compared to controls **(Fig. 7c, d).** This suggests that these TFs are involved in regulating lipid metabolism and that their KD may help reduce lipid buildup. Interestingly, we also observed that synapsin levels were increased specifically in the *Nfat KD* group, which could indicate a potential compensatory mechanism or a more pronounced effect on synaptic function when *Nfat* is KD **(Fig. 7e).**

Next, we first assessed the role of specific TFs in regulating AD risk genes and found distinct patterns of gene expression changes. Amphiphysin (Amph), Ephrin receptor (Eph), Ankyrin (Ank), Rho GTPase (Rho5), and Neuro-Laz (Nlaz) were specifically upregulated in *Vri KD*, suggesting that *Vri* may regulate these genes, potentially linking them to lipid metabolism and neuroinflammation. Conversely, Abca3, a gene involved in lipid transport, was found to be upregulated in the presence of Eip75b, *EcR*, and *Vri* KD, indicating that these TFs may co-regulate Abca3, expression. Additionally, cas family adaptor protein (P130CAS), a gene linked to cell adhesion and synaptic function, was affected in both Eip75b and *Vri* KD, suggesting that these TFs might also influence pathways regulating neuronal connectivity and function **(Fig. 7f)**.

Inhibition of Dgat2 led to reduced expression of Dgat2 transcription factors and AD risk genes in the *App^{NLG-F}* mouse model

To further validate these findings, we assessed TF expression in *App^{NLG-F}* mouse model and found that Nr1h1 (LXR), a TF involved in lipid regulation, was decreased in the presence of Dgat2 inhibitors, implying that Dgat2 inhibition alters lipid homeostasis at the transcriptional level. However, other TFs such as Srebf1 and Nfat5 remained unchanged, suggesting that Dgat2 inhibition selectively modulates specific lipid-regulating pathways without broadly affecting other TF (**Fig. 7g-i**). Moreover, in the *App^{NLG-F}* mouse model, the expression of key AD risk genes, Abca7, Rhbdf2, and cass4 was significantly reduced in the presence of Dgat2 inhibitors, suggesting that lipid metabolism modulation through Dgat2 inhibition could potentially reduce neuroinflammation and amyloid processing, two

critical aspects of AD pathogenesis. These findings suggest a complex relationship between lipid accumulation and synaptic regulation, with different Dgat2 TFs potentially playing distinct roles in lipid homeostasis and synaptic health.

Discussion

AD is characterized by the accumulation of amyloid plaques and tau tangles, leading to cognitive decline and neurodegeneration[38]. Genetic models, such as *Drosophila* expressing APP mutations, offer valuable insights into the mechanisms underlying AD[39]. In this study, we explored the effects of App^{NLG}, as well as the aggregation-prone β amyloid 42 (*Aβ42*), on locomotor function, memory, and lipid metabolism in *Drosophila.* Additionally, we examined the role of Diacylglycerol acyltransferase 2 (DGAT2), a key enzyme in lipid metabolism, through its knockdown and overexpression[40]. To further the established translational of our findings, we used the $App^{NLG\text{-}F}$ mouse model of AD, allowing for cross-species comparison of lipid profiles, neuroinflammation, and cognitive function. Through locomotor assays, cognitive tests, lipid analysis, and gene expression studies, we aimed to uncover how these genetic modifications influence AD pathogenesis and identify potential therapeutic strategies for mitigating AD-associated dysfunction.

Our findings highlight the complex interplay between amyloid pathology, lipid metabolism, and neuroinflammation across the species using the *Drosophila* and mouse AD models. In most assays, expression of *Aβ42* leads to more severe phenotypes compared to App^{NLG} (**Fig. 1b**). For example, we observed that male *Drosophila* expressing the *Aβ42* mutation exhibited significant locomotor impairments, as evidenced by reduced climbing ability in the geotaxis assay. Interestingly, the locomotor decline was more pronounced in the flies with panneuronal or glial-specific expression of *Aβ42* compared to those expressing the App^{NLG} construct, suggesting that the geotaxis phenotype is mutation specific **(Fig. 1b).** This is consistent with previous studies that have shown that amyloid-related motor deficits in *Drosophila* are associated with the expression of toxic *Aβ* species[41]. Additionally, our cognitive assays revealed a profound impairment in memory, particularly in flies expressing *Aβ42* in the mushroom bodies, a key brain region involved in olfactory learning. This observation underscores the critical role of specific brain regions in cognitive dysfunction in AD, aligning with findings in

mammalian models where amyloid pathology in the hippocampus and cortex leads to memory impairments[42]. Our study also highlights the important role of lipid metabolism in AD progression, as Dgat2 K*D* and OE modulated lipid dysregulation and synaptic function in both Drosophila and mouse models. Notably, the expression of AD risk genes was affected by Dgat2- modulation, further implicating lipid homeostasis as a key factor in neurodegeneration **(Fig. 1c-e).** These results provide compelling evidence that therapeutic strategies targeting lipid metabolism may offer a promising avenue for mitigating AD-related cognitive and locomotor dysfunctions.

Our findings demonstrate significant sleep disruptions in *Drosophila* models expressing the *Aβ42* mutation, particularly in terms of sleep fragmentation and altered sleep patterns. These disruptions were more pronounced compared to the APP mutation model, indicating that the *Aβ42* mutation has a stronger impact on sleep quality. The increase in total sleep time, predominantly during the nighttime **(Fig.2a),** aligns with previous research showing that AD models often exhibit prolonged sleep durations, especially at night[43, 44]. However, our results also revealed a notable rise in sleep fragmentation, particularly in the Elav- and GLaz-driven models, suggesting that while these flies sleep more, the quality of their sleep is impaired **(Fig.2c, d, f).** This phenomenon of fragmented sleep is consistent with clinical observations in AD patients, who often experience fragmented sleep despite longer sleep durations[45, 46]. The observed decrease in activity levels, particularly in the Elav-driven model, further supports the idea that these sleep changes are closely tied to disruptions in overall activity and circadian rhythms, which have been previously reported in both *Drosophila* and mammalian AD models[45, 47]. Additionally, the persistence of sleep disturbances in older flies suggests that sleep dysregulation may be a chronic feature of AD pathology, similar to the long-term sleep issues observed in AD patients[48, 49]. The differences in sleep fragmentation patterns between the neuronal and glial-specific models highlight the potential role of glial cells in modulating sleep, with glial-specific expression leading to a distinct pattern of increased daytime sleep bouts and longer bout lengths. This finding is in line with recent studies implicating glial activation in the disruption of sleep architecture in AD models[50-52]. Collectively, these results reinforce the idea that sleep disturbances, particularly

fragmented sleep, are a central feature of AD pathology and may serve as an early indicator of disease progression.

Evidence from our study provides that lipid dysregulation and synaptic impairment play crucial roles in the progression of AD, with distinct differences in the severity of these alterations between the *Aβ42 and App*^{NLG} models. Lipid accumulation, as indicated by lipid spot staining, was significantly elevated in both Drosophila and mouse models of AD, particularly in the *Aβ42* model, which exhibited more pronounced lipid deposition compared to the *App*^{NLG} model (**Fig. 3a, b, c, e**). This aligns with previous research indicating that dysregulated lipid metabolism, particularly the accumulation of lipid droplets, is a key feature of AD pathogenesi[53]. These lipid imbalances are thought to contribute to cellular stress and dysfunction, particularly in neurons and glial cells, which may exacerbate the cognitive and behavioral deficits seen in AD[55, 55]. In addition to lipid accumulation, we observed a marked reduction in synapsin expression, a protein crucial for synaptic function **(Fig. 3a, b, d, f).** This finding is consistent with studies showing that synaptic loss and dysfunction are hallmarks of AD, and are often correlated with cognitive decline[56, 57]. The more pronounced reductions in synapsin in the *Aβ42* model suggest that amyloid-β may have a more severe impact on synaptic integrity than other forms of amyloid precursor protein mutations, further supporting the idea that *Aβ42* plays a central role in synaptic dysfunction in AD[58]. Moreover, our transition to the *App*$^{NLG-F}$ mouse model corroborates these findings, as we observed a significant increase in lipid accumulation and glial activation, particularly with age, suggesting that lipid dysregulation and neuroinflammation are progressive features of AD pathology **(Fig. 3g, h, i, j; Extended Data Fig. 4g-j).** This is consistent with previous reports that aging exacerbates lipid accumulation and astrocyte activation in AD models[59]. The increase in GFAP expression, which is indicative of glial activation, further supports the idea that lipid imbalances are coupled with neuroinflammation in the aging brain, a crucial aspect of AD progression[60]. Together, these results reinforce the interconnectedness of lipid dysregulation, synaptic dysfunction, and neuroinflammation, highlighting their roles in the cognitive impairments characteristic of AD.

Microglial activation and neuroinflammation play pivotal roles in the progression of AD, as evidenced by the increased expression of Iba1, a marker for microglial activation,

in the App^{NLG-F} mouse model **(Fig. 4a, b).** This age-dependent upregulation of Iba1 suggests that chronic neuroinflammation becomes more pronounced with advancing age, which aligns with previous studies linking microglial activation to neurodegenerative diseases, including AD[61]**.** The increase in Iba1 expression is consistent with some reported literature indicating that sustained microglial activation is not merely a response to amyloid-beta accumulation, but rather a driver of neurodegeneration[62, 63]. Furthermore, the observed upregulation of Ptprq **(Fig. 4c)** further corroborates the presence of chronic, age-related inflammation in these mice, consistent with other reports on the role of neuroinflammation in AD pathology[64]. Interestingly, we found that not all inflammatory markers were elevated, suggesting selective pathways of microglial activation rather than a general inflammatory response. In addition to microglial activation, we detected increased expression of key AD risk genes, including Bin1, Rhbdf2, Apoe and Abca7, which are involved in amyloid processing and lipid metabolism **(Fig. 4c, d).** The upregulation of these genes with age further suggests an exacerbation of amyloid burden or disturbances in lipid metabolism, two critical aspects of AD pathology[65]**.** Furthermore, the elevation of Rhbdf2 and ApoE**,** both of which are linked to neuroinflammation and lipid homeostasis, underscores the role of disrupted lipid pathways in AD risk[66]**.** Collectively, these findings point to a progressive activation of inflammatory and amyloid-related pathways in the *App^{NLG-F}* model, with aging serving as a catalyst for the exacerbation of neuroinflammatory responses. The combination of these factors highlights the importance of neuroinflammation in driving disease progression in AD and suggests potential therapeutic avenues targeting these pathways.

The manipulation of *Dgat2* expression in our study sheds light on how lipid metabolism alterations may impact the neurodegenerative features of AD. *Dgat2*, a key enzyme involved in lipid biosynthesis, has previously been implicated in neuroinflammation and neurodegenerative processes[67, 68]. Our results, including both *Dgat2 KD* and OE in Drosophila models, indicate that lipid metabolism plays a critical role in influencing the locomotor, cognitive, and sleep-related deficits associated with AD. In line with previous studies, we observed that *Dgat2 KD* improves locomotor function, specifically in male flies expressing APP-mutant genes *(App^{NLG} and Aβ42),* where KD partially rescues climbing ability **(Fig. 5a).** This finding suggests that *Dgat2* inhibition may

mitigate some of the detrimental effects of amyloid-beta aggregation and could be protective against motor impairments seen in AD. Conversely, our results showed that *Dgat2* OE in the same AD models did not rescue locomotor deficits, but rather exacerbated them, supporting prior evidence that lipid accumulation is prevented through *Dgat2 KD*[70]. Cognitive function, measured through the olfactory aversion memory test, mirrored the locomotor results. The *Dgat2 KD* condition rescued memory impairment in both male and female AD models, while *Dgat2* OE did not yield similar improvements **(Fig. 5b, c).** This suggests that *Dgat2* modulation can influence cognitive function, with KD providing a potential protective effect in the context of AD. Interestingly, our sensory acuity test[69] further confirmed these trends, reinforcing the notion that *Dgat2* manipulation, particularly KD, can help preserve cognitive function in AD models. When assessing sleep patterns, we found that both *Dgat2* KD and OE conditions led to increased total sleep and reduced sleep fragmentation at 3 weeks of age **(Fig. 5d, e).** These results indicate that *Dgat2* manipulation does not drastically alter sleep behavior in younger flies, despite the differential effects on cognition and locomotion. This observation aligns with recent studies that show lipid metabolism disturbances can impact sleep, but the outcomes may be age-dependent[71]. However, in older AD flies (7wk), sleep patterns were largely unchanged by Dgat2 modulation, suggesting that the effects of lipid metabolism manipulation on sleep are less pronounced as the flies age **(Extended Data Fig. 9, 10a-c, 11a-d).** These findings highlight the complexity of lipid metabolism's role in neurodegenerative diseases, with age and disease progression influencing the extent of *Dgat2*'s impact on sleep, cognition, and motor function.

To better understand the effects of *Dgat2 KD* on lipid metabolism and neuroinflammation, we explored several key parameters in Drosophila and mouse models of AD. Our results demonstrate that *Dgat2* KD significantly reduces lipid accumulation, a hallmark of AD pathology, and increases synapsin levels, suggesting enhanced synaptic function **(Fig. 6a-c).** The improvement in synapsin expression supports the idea that altering lipid metabolism may lead to compensatory mechanisms aimed at preserving synaptic integrity, which aligns with findings showing that lipid dysregulation can impair synaptic plasticity and cognitive function in AD models[72]**.** These results provide compelling evidence that *Dgat2 KD* may reduce lipid-related pathologies and improve

synaptic function in AD models. In parallel, we assessed neuroinflammatory markers using qPCR and observed a significant reduction in the expression of Upd1 and Upd3, both of which are cytokines associated with neuroinflammation in AD **(Fig. 6d, e).** This reduction in inflammatory markers suggests that *Dgat2 KD* could mitigate neuroinflammation, a key feature of AD pathology. Interestingly, the expression of Dome and Hop receptors, which are integral to the JAK/STAT signaling pathway, remained unaffected, suggesting that the reduction in inflammation might not directly involve modulation of this pathway, but rather through other lipid-related mechanisms**.** This finding is consistent with the growing body of literature indicating that neuroinflammation in AD is complex and may not be solely mediated by the JAK/STAT pathway[73]**.** Further validation in the APP mouse model using a Dgat2 inhibitor revealed an increase in lipid spots, confirming the role of *Dgat2* in lipid accumulation **(Fig. 6f, g).** However, GFAP expression, a marker of astrocyte activation, remained unchanged **(Fig. 6h),** suggesting that *Dgat2* inhibition does not directly affect astrocyte-mediated neuroinflammation. Similarly, microglial activation, assessed through Iba1 expression, was unaffected by *Dgat2* inhibition (**Extended Data Fig. 13a, b).** This is in contrast to previous reports showing that lipid metabolism alterations can modulate both astrocytic and microglial responses in AD[74, 75]**.** While *Dgat2* inhibition did not directly affect microglia or astrocytes, we did observe a significant increase in Ptprq expression, a marker of inflammation, and a decrease in key AD risk genes, including Abca7, Cass4, and Rhbdf2 **(Fig. 6i),** highlighting a selective modulation of specific inflammatory pathways. These findings suggest that *Dgat2* modulation could offer a promising therapeutic strategy by simultaneously addressing lipid dysregulation and neuroinflammation in AD.

To explore the regulatory mechanisms underlying lipid dysregulation, neuroinflammation, and sleep dysfunctions in AD models, we focused on key TF that control *Dgat2* expression. Our results revealed significant upregulation of Eip75b, Nfat, and Srebp in Elav-driven AD models **(Fig. 7a),** suggesting that these TFs are involved in regulating lipid metabolism and cellular stress responses. This is consistent with recent findings indicating that transcriptional regulators, such as SREBP, play pivotal roles in lipid homeostasis and synaptic function in neurodegenerative diseases[76]. These TF, which are critical for cellular responses to stress and metabolic regulation, could therefore contribute

to AD pathophysiology by influencing lipid metabolism, synaptic function, and neuroinflammatory responses. Identifying the regulatory pathways controlled by these TFs will provide important insights into the molecular mechanisms driving AD-related dysfunctions and highlight potential therapeutic targets to address lipid imbalance and neuroinflammation in AD.

Further investigation into the impact of specific TF KDs on sleep activity revealed that sleep patterns were significantly altered in response to changes in *Dgat2* regulation. Both *EcR and Srebp KD* flies exhibited decreased total sleep, indicating that these transcription factors are critical for maintaining overall sleep duration **(Fig. 7b).** In contrast, *Eip75b KD* and *EcR KD* flies showed reduced daytime sleep, with *EcR KD* also uniquely affecting night sleep, emphasizing the distinct roles of these TFs in regulating sleep timing. These results are in line with previous research highlighting the influence of lipid metabolism on sleep regulation, with SREBP and EcR involved in modulating circadian rhythms and sleep architecture[76, 77.] Additionally, we observed reduced sleep fragmentation in the Nfat KD group, suggesting that Nfat plays a role in maintaining sleep stability, while increased day sleep fragmentation in *Eip75b and Srebp KD* flies points to their involvement in regulating sleep continuity during the day. The effects of Dgat2 modulation on sleep fragmentation align with previous studies indicating that lipid metabolic pathways are intricately connected to sleep homeostasis and stability in neurodegenerative models[78]. Taken together, these findings demonstrate that distinct TF regulating Dgat2 expression play important roles in shaping various aspects of sleep, providing deeper insights into the molecular mechanisms driving sleep disturbances in AD.

Over all, as mentioned in Fig.8, both panneuronal and glial-specific expression of *App^{NLG} and Aβ42* resulted in notable impairments in locomotor and cognitive performance, along with enhanced lipid accumulation and decreased synapsin levels. These detrimental effects were partially rescued by Dgat KD, as indicated by the up and down arrows, highlighting a potential therapeutic role for Dgat inhibition in mitigating neurodegeneration in *Drosophila.* The bottom panel further explores the molecular markers involved in this process, showing altered expression patterns of glial and neuronal proteins, such as Gfap, Ib1, Dgat2, and Adrp, in both young and old *App^{NLG-F}* mice. Additionally, the data illustrate the impact of Dgat2 inhibitors on these markers,

providing insight into the role of Dgat2 in modulating glial activation, lipid accumulation, and neurodegenerative changes in the *App*$^{NLG\text{-}F}$ mouse model.

Funding: This work was partially supported by National Institutes of Health (NIH) grants AG065992 and RF1NS133378 to G.C.M. P30 AG050886 (GM and JZ), R01AG072895 (JZ), R01ES034846 (JZ), R21AG081687 (JZ). This work is also supported by UAB Startup funds 3123226 and 3123227 to G.C.M.

Author Contribution: GCM, JZ, JK, XO, and AY designed the experiments including feedback from JJ. AY performed most sleep and all geotaxis experiments. AY performed the analysis of sleep parameters, qPCR experiments, and analysis of both *Drosophila* and mouse samples. OX performed all immunofluorescence staining of mouse brain samples. MB performed most memory assays. JCW processes all brain samples of the *Drosophila* brain and performs immunofluorescence staining and analyses with help from GCM. KM collected some sleep activity and memory data and performed immunoblot analyses. JC has performed Dgat2 inhibitor dosing in mice. AY performed analysis and analyzed all the data including statistical analyses with help from GCM and JZ. AY prepared the paper with GCM's input. All the authors reviewed the manuscript and provided their feedback.

Acknowledgment: Stocks obtained from the Bloomington Drosophila Stock Center were used in this study.

Competing interests: The authors declare no competing interests.

Additional Information: Extended data is available for this paper at available in a separate PDF file

Data source file: Source data is available for this paper at source data in a single Excel sheet.

Online Data Sharing: NA

References

1. Western, Daniel, et al. "Proteogenomic analysis of human cerebrospinal fluid identifies neurologically relevant regulation and implicates causal proteins for Alzheimer's disease." *Nature Genetics* (2024): 1-13.
2. Nichols, Emma, et al. "Estimation of the global prevalence of dementia in 2019 and forecasted prevalence in 2050: an analysis for the Global Burden of Disease Study 2019." *The Lancet Public Health* 7.2 (2022): e105-e125.
3. Bartoletti-Stella, Anna, et al. "Identification of rare genetic variants in Italian patients with dementia by targeted gene sequencing." *Neurobiology of Aging* 66 (2018): 180-e23.
4. Uddin, Md Sahab, et al. "Revisiting the role of brain and peripheral Aβ in the pathogenesis of Alzheimer's disease." *Journal of the Neurological Sciences* 416 (2020): 116974.
5. Nikom, David, and Sika Zheng. "Alternative splicing in neurodegenerative disease and the promise of RNA therapies." *Nature Reviews Neuroscience* 24.8 (2023): 457-473.
6. Yang, Danying, et al. "Lipid metabolism and storage in neuroglia: role in brain development and neurodegenerative diseases." *Cell & Bioscience* 12.1 (2022): 106.
7. Ralhan, Isha, et al. "Lipid droplets in the nervous system." *Journal of Cell Biology* 220.7 (2021): e202102136.
8. Wong, Matthew W., et al. "Dysregulation of lipids in Alzheimer's disease and their role as potential biomarkers." *Alzheimer's & Dementia* 13.7 (2017): 810-827.
9. Martens, Yuka A., et al. "ApoE Cascade Hypothesis in the pathogenesis of Alzheimer's disease and related dementias." *Neuron* 110.8 (2022): 1304-1317.
10. Picard, Cynthia, et al. "Alterations in cholesterol metabolism–related genes in sporadic Alzheimer's disease." *Neurobiology of aging* 66 (2018): 180-e1.
11. Chen, Feng, et al. "The vascular contribution of apolipoprotein E to Alzheimer's disease." *Brain* (2024): awae156.
12. Singh, Rajat, and Ana Maria Cuervo. "Lipophagy: connecting autophagy and lipid metabolism." *International journal of cell biology* 2012.1 (2012): 282041.

13. Ates, Gamze, et al. "CMS121, a fatty acid synthase inhibitor, protects against excess lipid peroxidation and inflammation and alleviates cognitive loss in a transgenic mouse model of Alzheimer's disease." *Redox Biology* 36 (2020): 101648.
14. Daugherty, Daniel, et al. "A novel Alzheimer's disease drug candidate targeting inflammation and fatty acid metabolism." *Alzheimer's Research & Therapy* 9 (2017): 1-17.
15. Ioannou, Maria S., et al. "Neuron-astrocyte metabolic coupling protects against activity-induced fatty acid toxicity." *Cell* 177.6 (2019): 1522-1535.
16. Eraso-Pichot, Abel, et al. "GSEA of mouse and human mitochondriomes reveals fatty acid oxidation in astrocytes." *Glia* 66.8 (2018): 1724-1735.
17. Edmond, J., et al. "Capacity for substrate utilization in oxidative metabolism by neurons, astrocytes, and oligodendrocytes from developing brain in primary culture." *Journal of neuroscience research* 18.4 (1987): 551-561.
18. Namgaladze, Dmitry, and Bernhard Brüne. "Macrophage fatty acid oxidation and its roles in macrophage polarization and fatty acid-induced inflammation." *Biochimica et Biophysica Acta (BBA)-Molecular and Cell Biology of Lipids* 1861.11 (2016): 1796-1807.
19. Song, Gyun Jee, and Kyoungho Suk. "Pharmacological modulation of functional phenotypes of microglia in neurodegenerative diseases." *Frontiers in aging neuroscience* 9 (2017): 139.
20. Liu, Bingrun, et al. "Isovitexin-mediated regulation of microglial polarization in lipopolysaccharide-induced neuroinflammation via activation of the CaMKKβ/AMPK-PGC-1α signaling axis." *Frontiers in immunology* 10 (2019): 2650.
21. Leng, Fangda, and Paul Edison. "Neuroinflammation and microglial activation in Alzheimer disease: where do we go from here?." *Nature Reviews Neurology* 17.3 (2021): 157-172.
22. Daynes, Raymond A., and Dallas C. Jones. "Emerging roles of PPARs in inflammation and immunity." *Nature Reviews Immunology* 2.10 (2002): 748-759.

23. Adamovich, Yaarit, et al. "Circadian clocks and feeding time regulate the oscillations and levels of hepatic triglycerides." *Cell metabolism* 19.2 (2014): 319-330.
24. Moraes, Ruan CM, et al. "Apolipoprotein E Induces Lipid Accumulation Through Dgat2 That Is Prevented with Time-Restricted Feeding in Drosophila." *Genes* 15.11 (2024): 1376.
25. Livelo, Christopher, et al. "Time-restricted feeding mediated modulation of microbiota leads to changes in muscle physiology in Drosophila obesity models." *Aging Cell* (2024): e14382.
26. Livelo, Christopher, et al. "Time-restricted feeding promotes muscle function through purine cycle and AMPK signaling in Drosophila obesity models." *Nature communications* 14.1 (2023): 949.
27. Prakash, Priya, et al. "Amyloid β induces lipid droplet-mediated microglial dysfunction in Alzheimer's disease." *bioRxiv* (2023).
28. Panda, Satchidananda, John B. Hogenesch, and Steve A. Kay. "Circadian rhythms from flies to human." *Nature* 417.6886 (2002): 329-335.
29. Hardin, Paul E., and Satchidananda Panda. "Circadian timekeeping and output mechanisms in animals." *Current opinion in neurobiology* 23.5 (2013): 724-731.
30. Austad, Steven N., et al. "Targeting whole body metabolism and mitochondrial bioenergetics in the drug development for Alzheimer's disease." *Acta Pharmaceutica Sinica B* 12.2 (2022): 511-531.
31. Villanueva, Jesús E., et al. "Time-restricted feeding restores muscle function in Drosophila models of obesity and circadian-rhythm disruption." *Nature communications* 10.1 (2019): 2700.
32. Duncan, M. J., et al. "Restricting feeding to the active phase in middle-aged mice attenuates adverse metabolic effects of a high-fat diet." *Physiology & behavior* 167 (2016): 1-9.
33. Melkani, Girish C., et al. "Huntington's disease induced cardiac amyloidosis is reversed by modulating protein folding and oxidative stress pathways in the Drosophila heart." *PLoS genetics* 9.12 (2013): e1004024.

34. Gill, Shubhroz, et al. "Time-restricted feeding attenuates age-related cardiac decline in Drosophila." *Science* 347.6227 (2015): 1265-1269.
35. Villanueva, Jesús E., et al. "Time-restricted feeding restores muscle function in Drosophila models of obesity and circadian-rhythm disruption." *Nature communications* 10.1 (2019): 2700.
36. Livelo, Christopher, et al. "Time-restricted feeding promotes muscle function through purine cycle and AMPK signaling in Drosophila obesity models." *Nature communications* 14.1 (2023): 949.
37. Thrupp, Nicola, Bart De Strooper, and Mark Fiers. "Transcriptomics to study the cellular phase of Alzheimer's Disease." (2023).
38. Zhang, Huiqin, et al. "Interaction between Aβ and tau in the pathogenesis of Alzheimer's disease." *International journal of biological sciences* 17.9 (2021): 2181.
39. Padmanabhan, Pranesh, and Jürgen Götz. "Clinical relevance of animal models in aging-related dementia research." *Nature Aging* 3.5 (2023): 481-493.
40. Rong, Shunxing, et al. "DGAT2 inhibition blocks SREBP-1 cleavage and improves hepatic steatosis by increasing phosphatidylethanolamine in the ER." *Cell metabolism* 36.3 (2024): 617-629.
41. Sun, Zhen-Dong, et al. "Toxicities of amyloid-beta and tau protein are reciprocally enhanced in the Drosophila model." *Neural regeneration research* 17.10 (2022): 2286-2292.
42. Polis, Baruh, and Abraham O. Samson. "Addressing the Discrepancies Between Animal Models and Human Alzheimer’s Disease Pathology: Implications for Translational Research." *Journal of Alzheimer's Disease* Preprint (2024): 1-20.
43. Meyer, Nicholas, et al. "Circadian rhythms and disorders of the timing of sleep." *The Lancet* 400.10357 (2022): 1061-1078.
44. Insel, Philip S., et al. "Association of sleep and β-amyloid pathology among older cognitively unimpaired adults." *JAMA Network Open* 4.7 (2021): e2117573-e2117573.

45. Duncan, M. J., et al. "Chronic fragmentation of the daily sleep-wake rhythm increases amyloid-beta levels and neuroinflammation in the 3xTg-AD mouse model of Alzheimer's disease." *Neuroscience* 481 (2022): 111-122.
46. Winer, Joseph R., et al. "Association of short and long sleep duration with amyloid-β burden and cognition in aging." *JAMA neurology* 78.10 (2021): 1187-1196.
47. Majcin Dorcikova, Michaëla, et al. "Circadian clock disruption promotes the degeneration of dopaminergic neurons in male Drosophila." *Nature Communications* 14.1 (2023): 5908.
48. Peter-Derex, Laure, et al. "Sleep and Alzheimer's disease." *Sleep medicine reviews* 19 (2015): 29-38.
49. Minakawa, Eiko N., et al. "Chronic sleep fragmentation exacerbates amyloid β deposition in Alzheimer's disease model mice." *Neuroscience letters* 653 (2017): 362-369.
50. Bellesi, Michele, et al. "Sleep loss promotes astrocytic phagocytosis and microglial activation in mouse cerebral cortex." *Journal of Neuroscience* 37.21 (2017): 5263-5273.
51. Garofalo, Stefano, et al. "Role of glia in the regulation of sleep in health and disease." *Compr. Physiol* 10.2 (2020): 687-712.
52. Gentry, Nicholas W., et al. "Microglia are involved in the protection of memories formed during sleep deprivation." *Neurobiology of Sleep and Circadian Rhythms* 12 (2022): 100073.
53. Liu, Yue, et al. "Plasma lipidome is dysregulated in Alzheimer's disease and is associated with disease risk genes." *Translational psychiatry* 11.1 (2021): 344.
54. Fan, Yong-Gang, et al. "Vitamin D deficiency exacerbates Alzheimer-like pathologies by reducing antioxidant capacity." *Free Radical Biology and Medicine* 161 (2020): 139-149.
55. Keeney, Jeriel TR, et al. "Dietary vitamin D deficiency in rats from middle to old age leads to elevated tyrosine nitration and proteomics changes in levels of key proteins in brain: implications for low vitamin D-dependent age-related cognitive decline." *Free Radical Biology and Medicine* 65 (2013): 324-334.

56. Lan, Guoyu, et al. "Association of presynaptic loss with Alzheimer's disease and cognitive decline." *Annals of Neurology* 92.6 (2022): 1001-1015.
57. Saroja, Sivaprakasam R., et al. "Differential expression of tau species and the association with cognitive decline and synaptic loss in Alzheimer's disease." *Alzheimer's & Dementia* 18.9 (2022): 1602-1615.
58. Piccoli, Tommaso, et al. "Biomarkers related to synaptic dysfunction to discriminate alzheimer’s disease from other neurological disorders." *International Journal of Molecular Sciences* 23.18 (2022): 10831.
59. Emre, Ceren, et al. "Age-related changes in brain phospholipids and bioactive lipids in the APP knock-in mouse model of Alzheimer’s disease." *Acta neuropathologica communications* 9.1 (2021): 116.]
60. Emre, Ceren, et al. "Age-related changes in brain phospholipids and bioactive lipids in the APP knock-in mouse model of Alzheimer’s disease." *Acta neuropathologica communications* 9.1 (2021): 116.
61. Schuitemaker, Alie, et al. "Microglial activation in healthy aging." *Neurobiology of aging* 33.6 (2012): 1067-1072.
62. Kinney, Jefferson W., et al. "Inflammation as a central mechanism in Alzheimer's disease." *Alzheimer's & Dementia: Translational Research & Clinical Interventions* 4 (2018): 575-590.
63. Agrawal, Ishan, and Sushmita Jha. "Mitochondrial dysfunction and Alzheimer’s disease: Role of microglia." *Frontiers in aging neuroscience* 12 (2020): 559682.
64. Sakuraba, Juichi, et al. "Substrate specificity of R3 receptor-like protein-tyrosine phosphatase subfamily toward receptor protein-tyrosine kinases." *Journal of Biological Chemistry* 288.32 (2013): 23421-23431.
65. Prendecki, Michał, et al. "Genetic factors related to the immune system in subjects at risk of developing Alzheimer's disease." *Journal of Integrative Neuroscience* 19.2 (2020): 359-371.
66. De Jager, Philip L., et al. "Alzheimer's disease: early alterations in brain DNA methylation at ANK1, BIN1, RHBDF2 and other loci." *Nature neuroscience* 17.9 (2014): 1156-1163.

67. Stone, Scot J., et al. "The endoplasmic reticulum enzyme DGAT2 is found in mitochondria-associated membranes and has a mitochondrial targeting signal that promotes its association with mitochondria." *Journal of Biological Chemistry* 284.8 (2009): 5352-5361.
68. Kang, Jihong, and Serge Rivest. "Lipid metabolism and neuroinflammation in Alzheimer's disease: a role for liver X receptors." *Endocrine reviews* 33.5 (2012): 715-746.
69. Meschi, Eleonora, et al. "Compensatory enhancement of input maintains aversive dopaminergic reinforcement in hungry Drosophila." *Neuron* (2024).
70. Moraes, Ruan CM, et al. "Apolipoprotein E Induces Lipid Accumulation Through Dgat2 That Is Prevented with Time-Restricted Feeding in Drosophila." *Genes* 15.11 (2024): 1376.
71. Broussard, Josiane, and Matthew J. Brady. "The impact of sleep disturbances on adipocyte function and lipid metabolism." *Best Practice & Research Clinical Endocrinology & Metabolism* 24.5 (2010): 763-773.
72. Kao, Yu-Chia, et al. "Lipids and Alzheimer's disease." *International journal of molecular sciences* 21.4 (2020): 1505.
73. Jain, Mayank, et al. "Role of JAK/STAT in the neuroinflammation and its association with neurological disorders." *Annals of neurosciences* 28.3-4 (2021): 191-200.
74. Iglesias, José, Ludis Morales, and George E. Barreto. "Metabolic and inflammatory adaptation of reactive astrocytes: role of PPARs." *Molecular neurobiology* 54 (2017): 2518-2538.
75. Marschallinger, Julia, et al. "Lipid-droplet-accumulating microglia represent a dysfunctional and proinflammatory state in the aging brain." *Nature neuroscience* 23.2 (2020): 194-208.
76. Ang, Mary Jasmin, and Changjong Moon. "SREBP and central nervous system disorders: genetic overlaps revealed by in silico analysis." *Journal of Integrative Neuroscience* 21.3 (2022): 95.
77. Li, Yongjun, et al. "Ecdysone acts through cortex glia to regulate sleep in Drosophila." *Elife* 12 (2023): e81723.

78. Guo, Yiming, et al. "Diurnal expression of Dgat2 induced by time-restricted feeding maintains cardiac health in the Drosophila model of circadian disruption." *Aging Cell* (2024): e14169.
79. Shie, Feng-Shiun, et al. "Diet-induced hypercholesterolemia enhances brain Aβ accumulation in transgenic mice." Neuroreport 13.4 (2002): 455-459.
80. Refolo, Lorenzo M., et al. "Hypercholesterolemia accelerates the Alzheimer's amyloid pathology in a transgenic mouse model." *Neurobiology of disease* 7.4 (2000): 321-331.
81. Bellenguez, Céline, et al. "New insights into the genetic etiology of Alzheimer's disease and related dementias." *Nature genetics* 54.4 (2022): 412-436.
82. De Rojas, Itziar, et al. "Common variants in Alzheimer's disease and risk stratification by polygenic risk scores." *Nature communications* 12.1 (2021): 3417.
83. Huang, Helen Xuexia, et al. "Mass spectrometry imaging highlights dynamic patterns of lipid co-expression with Aβ plaques in mouse and human brains." *Journal of Neurochemistry* (2024).
84. Yenilmez, Batuhan, et al. "An RNAi therapeutic targeting hepatic DGAT2 in a genetically obese mouse model of nonalcoholic steatohepatitis." Molecular Therapy 30.3 (2022): 1329-1342.
85. Rong, Shunxing, et al. "DGAT2 inhibition blocks SREBP-1 cleavage and improves hepatic steatosis by increasing phosphatidylethanolamine in the ER." Cell metabolism 36.3 (2024): 617-629.
86. Munkácsy, Erin, et al. "Neuronal-specific proteasome augmentation via Prosβ5 overexpression extends lifespan and reduces age-related cognitive decline." Aging cell 18.5 (2019): e13005.
87. Chocron, E. Sandra, et al. "Genetic and pharmacologic proteasome augmentation ameliorates Alzheimer's-like pathology in mouse and fly APP overexpression models." Science advances 8.23 (2022): eabk2252.
88. Watson, J., Roth, J. R., Melkani, G. C. Direct Cryosectioning of Drosophila Heads for Enhanced Brain Fluorescence Staining and Immunostaining. J. Vis. Exp. (Pending Publication), e67791, In-press (2025).

89. Roth, Jonathan R., et al. "Rapamycin reduces neuronal mutant huntingtin aggregation and ameliorates locomotor performance in Drosophila." Frontiers in Aging Neuroscience 15 (2023): 1223911.
90. Hoedjes, Katja M., et al. "A single nucleotide variant in the PPARγ-homolog Eip75B affects fecundity in Drosophila." Molecular biology and evolution 40.2 (2023): msad018.
91. Uyehara, Christopher M., and Daniel J. McKay. "Direct and widespread role for the nuclear receptor EcR in mediating the response to ecdysone in Drosophila." Proceedings of the National Academy of Sciences 116.20 (2019): 9893-9902.
92. Yang, Teddy TC, et al. "Role of transcription factor NFAT in glucose and insulin homeostasis." Molecular and cellular biology 26.20 (2006): 7372-7387.
93. Rong, Shunxing, et al. "DGAT2 inhibition blocks SREBP-1 cleavage and improves hepatic steatosis by increasing phosphatidylethanolamine in the ER." Cell metabolism 36.3 (2024): 617-629.
94. Yokoyama, Miyabishara, et al. "Mouse models of Alzheimer’s disease." Frontiers in Molecular Neuroscience 15 (2022): 912995.
95. Koushika, Sandhya P., Michael J. Lisbin, and Kalpana White. "ELAV, a Drosophila neuron-specific protein, mediates the generation of an alternatively spliced neural protein isoform." Current Biology 6.12 (1996): 1634-1641.
96. Sanchez, Diego, et al. "Loss of glial lazarillo, a homolog of apolipoprotein D, reduces lifespan and stress resistance in Drosophila." Current Biology 16.7 (2006): 680-686.
97. Aso, Yoshinori, et al. "The mushroom body of adult Drosophila characterized by GAL4 drivers." Journal of neurogenetics 23.1-2 (2009): 156-172.
98. Osterwalder, Thomas, et al. "A conditional tissue-specific transgene expression system using inducible GAL4." Proceedings of the National Academy of Sciences 98.22 (2001): 12596-12601.
99. Whittaker, Daniel S., et al. "Circadian modulation by time-restricted feeding rescues brain pathology and improves memory in mouse models of Alzheimer’s disease." Cell metabolism 35.10 (2023): 1704-1721.

100. King, Melvin W., Yining Chen, and Erik S. Musiek. "Time-restricted feeding and Alzheimer’s disease: you are when you eat." Trends in Molecular Medicine (2023).
101. Hendricks, Joan C., et al. "Rest in Drosophila is a sleep-like state." Neuron 25.1 (2000): 129-138.

Fig.1

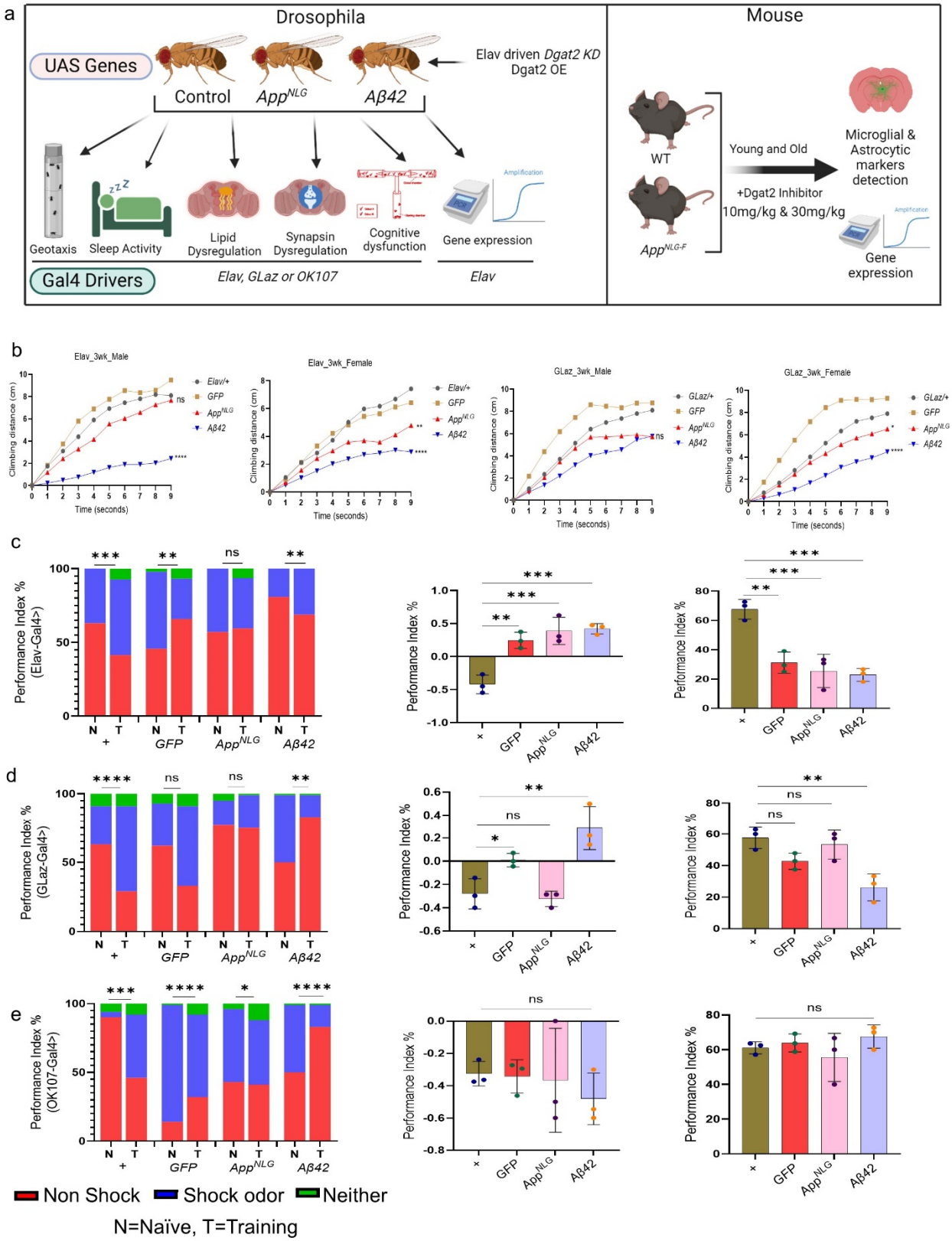
a
Drosophila
Mouse
UAS Genes
Control
App^NLG
Aβ42
Elav driven Dgat2 KD
Dgat2 OE
Geotaxis
Sleep Activity
Lipid Dysregulation
Synapsin Dysregulation
Cognitive dysfunction
Gene expression
Gal4 Drivers
Elav, GLaz or OK107
Elav
WT
App^NLG-F
Young and Old
+Dgat2 Inhibitor
10mg/kg & 30mg/kg
Microglial & Astrocytic markers detection
Gene expression
b
Elav_3wk_Male
Elav_3wk_Female
GLaz_3wk_Male
GLaz_3wk_Female
Climbing distance (cm)
Time (seconds)
Elav/+
GFP
App^NLG
Aβ42
GLaz/+
c
Performance Index % (Elav-Gal4>)
d
Performance Index % (GLaz-Gal4>)
e
Performance Index % (OK107-Gal4>)
N T
+
GFP
App^NLG
Aβ42
Non Shock
Shock odor
Neither
N=Naïve, T=Training

Fig.1| Panneuronal and glial-specific expression of *App^{NLG} and Aβ42* led to compromised locomotor and cognitive performance. a, Flow chart depicting the experimental setup. Each UAS gene was crossed with the region-specific Gal-4 drivers. To explore the contribution of Dgat2 in *Aβ42 and App* accumulation, we performed Elav-driven *Dgat2 KD* and Dgat2 OE in *Drosophila* and used an *App^{NLG-F}* mouse model with Dgat2 inhibitor**. b,** Negative geotaxis assay of Elav and GLaz drove A*pp^{NLG} and Aβ42* models in 3wk males and females**. c-e,** Memory assay of *Drosophila*: Original method, the difference between fly decisions, flies avoiding shock odor in Elav, GLaz and OK107 *App^{NLG} and Aβ42* models. Two-way ANOVA with multiple comparisons done with Uncorrected Fisher's LSD test was performed for geotaxis, n=3 replicates per group and each group had 10 flies. Chi-square tests were performed for memory assay, (*App^{NLG} N=50, Aβ42=46, W^{1118}=54, GFP=45*). *P<0.05, **P<0.01 and ***P<0.001 n.s = not significant. Exact p values are provided in the source data.

Fig.2

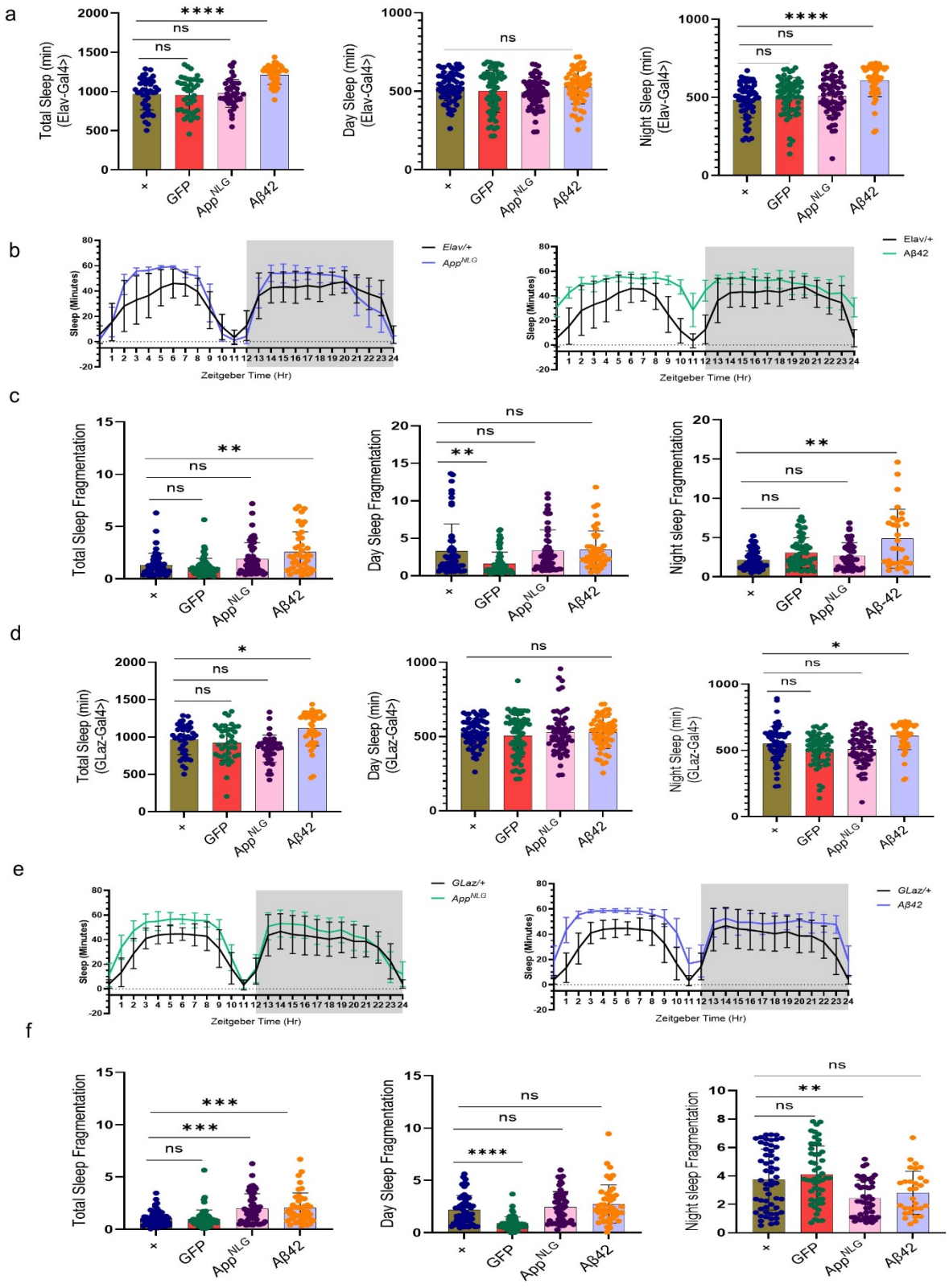
a
Total Sleep (min) (Elav-Gal4>)
Day Sleep (min) (Elav-Gal4>)
Night Sleep (min) (Elav-Gal4>)
****
ns
b
Sleep (Minutes)
Zeitgeber Time (Hr)
Elav/+
AppNLG
Aβ42
c
Total Sleep Fragmentation
Day Sleep Fragmentation
Night sleep Fragmentation
**
d
Total Sleep (min) (GLaz-Gal4>)
Day Sleep (min) (GLaz-Gal4>)
Night Sleep (min) (GLaz-Gal4>)
*
e
GLaz/+
Aβ42
f
***
****

Fig. 2 | Panneuronal and glial-specific expression of A*β42* has compromised circadian activity and sleep quality compared to *App^{NLG}* which worsens with age

a, Total, day and night sleep (in minutes) in Elav-driven *APP/aβ* Models. **b,** Sleep profiles at different zeitgeber time (hr.) in Elav-driven AD models only compared to their respective controls. **c,** Total, day and night sleep fragmentation in Elav-driven *APP/aβ* Models. **d,** Total, day and night sleep in (in minutes) in GLaz-driven APP/aβ Models. **e,** Sleep profiles at different zeitgeber time (hr.) in GLaz-driven AD models only compared to their respective controls. **f,** Total, day and night sleep fragmentation in GLaz-driven *APP/aβ* models. All experiments were performed in 3-week-old males only. Non-parametric One-way ANOVA with multiple comparisons done with the Kruskal Wallis test was performed for sleep activity and sleep fragmentation. Each dot represents several flies *(App^{NLG} N=64, Aβ42=60, W^{1118}=64, GFP=60)* *p < .05; **p < .01; ***p < .001; ns = not significant. Exact p values are provided in the source data.

Fig.3

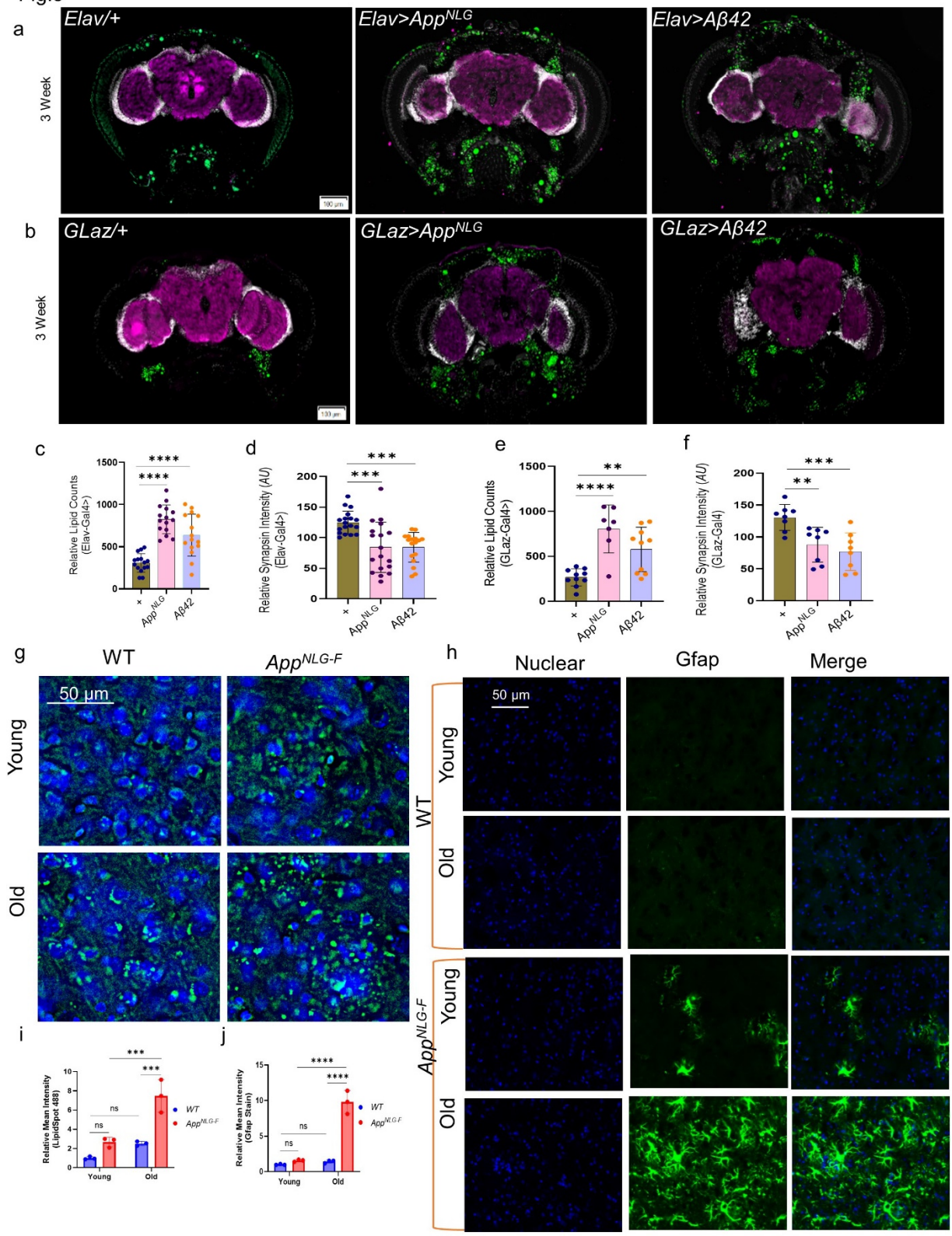
a
Elav/+
Elav>App^NLG
Elav>Aβ42
3 Week
b
GLaz/+
GLaz>App^NLG
GLaz>Aβ42
3 Week
c
Relative Lipid Counts (Elav-Gal4>)
d
Relative Synapsin Intensity (AU) (Elav-Gal4>)
e
Relative Lipid Counts (GLaz-Gal4>)
f
Relative Synapsin Intensity (AU) (GLaz-Gal4)
+
App^NLG
Aβ42
g
WT
App^NLG-F
Young
Old
50 μm
h
Nuclear
Gfap
Merge
WT
App^NLG-F
Young
Old
50 μm
i
Relative Mean Intensity (LipidSpot 488)
j
Relative Mean Intensity (Gfap Stain)
WT
App^NLG-F
Young
Old
ns

Fig. 3 | *App^{NLG} and Aβ42* induce lipid accumulation and synapsin reduction in Drosophila, while *App^{NLG-F}* mice show cortical lipid build-up and astrocyte activation. a-b, Representative image showing the expression of lipid accumulation (green), synaptic loss (purple), a marker of neurodegeneration, and DAPI (white) in the brains of Elav and GLaz driven *App^{NLG} and Aβ42* flies**. c-f,** Quantification of the expression level of lipid counts and synapsin intensity in Elav and GLaz driven *APP^{NLG} and Aβ42* flies. All experiments were performed in 3-week-old flies. **g,** Representative image showing the expression of lipid spot (green), a marker of lipid accumulation, and DAPI (blue) in the mouse brains of young and old wild type and App^{NLG-F} models. **h,** Representative image showing the expression of Gfap a marker of astrocyte activation, and DAPI (blue) in the mouse brains of young and old wild type and App knock-in models**. i-j,** Quantification of the expression level of lipid spots and relative mean intensity of Gfap. All data were presented as mean ± SD., with n=3 mice per group and 5-6 flies per group. Fold changes of fluorescence intensity were calculated relative to controls. One-way ANOVA with Turkey's multiple comparisons test was performed for flies' data and Two-way ANOVA with multiple comparisons done with Uncorrected Fisher's LSD test was performed for mouse data. *$p < .05$; **$p < .01$; ***$p < .001$; ns = not significant. Exact p values are provided in the source data.

Fig.4

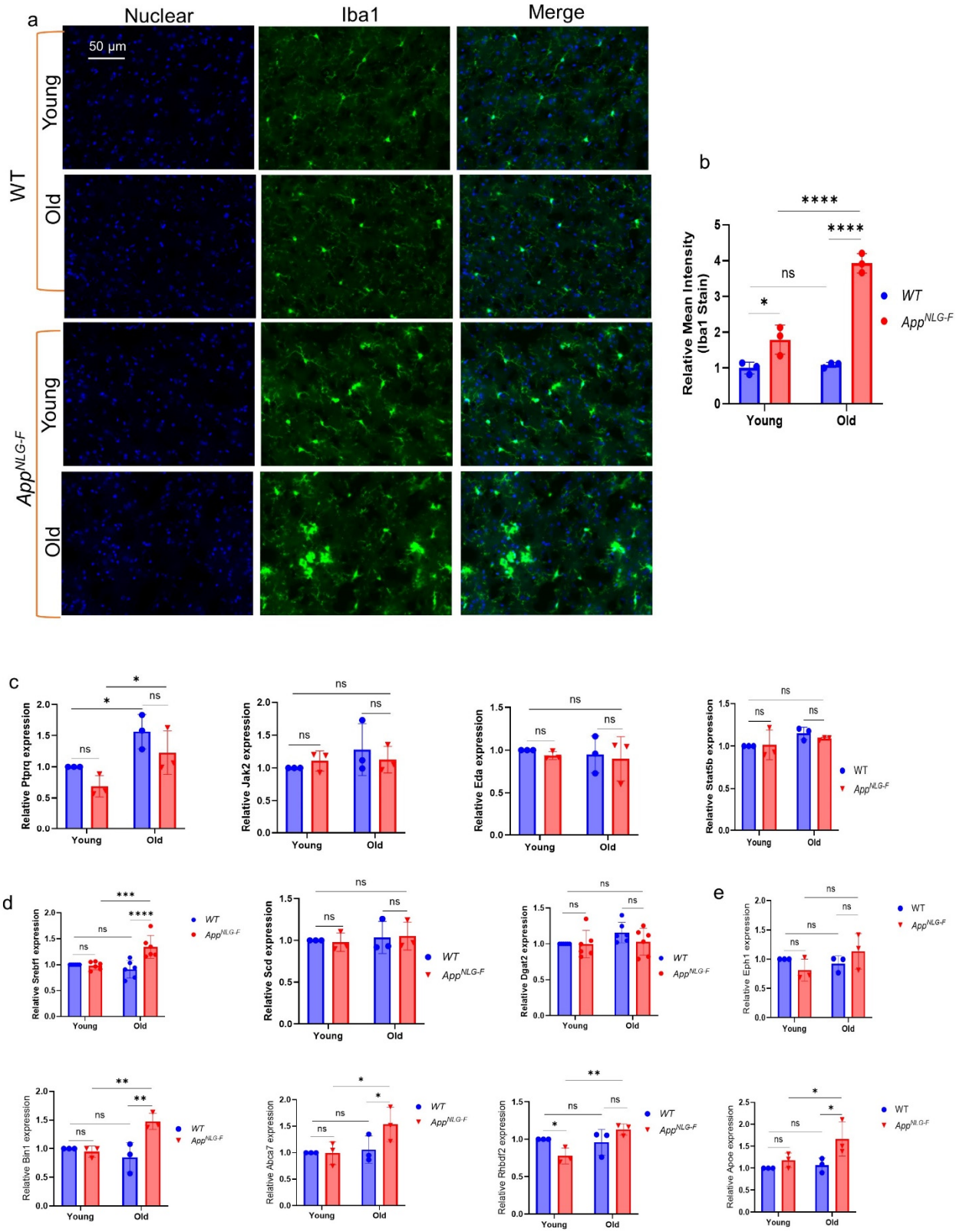
a
Nuclear
Iba1
Merge
50 μm
WT
Young
Old
App^NLG-F
Young
Old
b
Relative Mean Intensity (Iba1 Stain)
Young
Old
WT
App^NLG-F
c
Relative Ptprq expression
Relative Jak2 expression
Relative Eda expression
Relative Stat5b expression
d
Relative Srebf1 expression
Relative Scd expression
Relative Dgat2 expression
e
Relative Eph1 expression
Relative Bin1 expression
Relative Abca7 expression
Relative Rhbdf2 expression
Relative Apoe expression

Fig. 4 | Age-dependent increase in neuroinflammation and AD risk gene expression in a mouse model of *App*$^{NLG-F}$. a, Immunofluorescence staining showing the expression level of Iba1 protein in microglia within the cortex region of the brain of WT and *App*$^{NLG-F}$ mouse model at young and old age. **b,** Quantification of the Iba1 expression level in microglia in a; n=3 mice per group. **c-e,** Relative expression level of inflammatory genes**,** metabolic gene markers**,** and AD risk genes**,** in young and old WT and *App*$^{NLG-F}$ mouse models. Two-way ANOVA with multiple comparisons done with Uncorrected Fisher's LSD test was performed. *p < .05; **p < .01; ***p < .001; ns = not significant. Exact p values are provided in the source data.

Fig.5

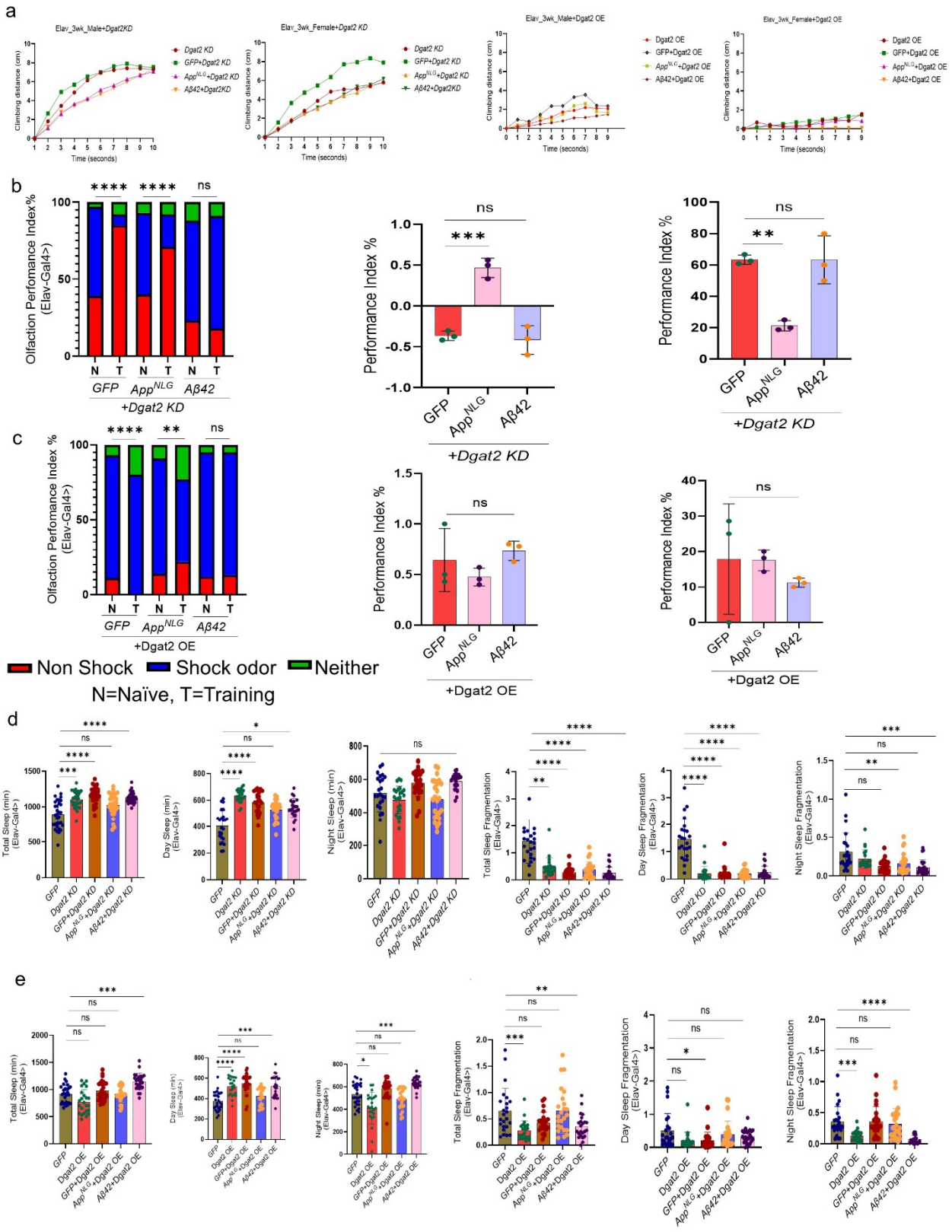
a
Elav_3wk_Male+Dgat2KD
Elav_3wk_Female+Dgat2 KD
Elav_3wk_Male+Dgat2 OE
Elav_3wk_Female+Dgat2 OE
Climbing distance (cm)
Time (seconds)
Dgat2 KD
GFP+Dgat2 KD
App^NLG+Dgat2 KD
Aβ42+Dgat2KD
Dgat2 OE
GFP+Dgat2 OE
App^NLG+Dgat2 OE
Aβ42+Dgat2 OE
b
Olfaction Perfomance Index% (Elav-Gal4>)
N T N T N T
GFP App^NLG Aβ42
+Dgat2 KD
Performance Index %
GFP App^NLG Aβ42
+Dgat2 KD
c
Olfaction Perfomance Index % (Elav-Gal4>)
+Dgat2 OE
Non Shock
Shock odor
Neither
N=Naïve, T=Training
d
Total Sleep (min) (Elav-Gal4>)
Day Sleep (min) (Elav-Gal4>)
Night Sleep (min) (Elav-Gal4>)
Total Sleep Fragmentation (Elav-Gal4>)
Day Sleep Fragmentation (Elav-Gal4>)
Night Sleep Fragmentation (Elav-Gal4>)
GFP Dgat2 KD GFP+Dgat2 KD App^NLG+Dgat2 KD Aβ42+Dgat2 KD
e
GFP Dgat2 OE GFP+Dgat2 OE App^NLG+Dgat2 OE Aβ42+Dgat2 OE

Fig.5| Dgat2 KD enhances locomotor and cognitive performance, restores sleep activity, and reduces fragmentation linked to *App^{NLG} and Aβ42* expression.

a, Negative geotaxis assay of Elav driven *Dgat2 KD* and OE in AD models in 3wk male and female**. b-c,** Memory assay of Drosophila: original method, difference between fly decisions, flies avoiding shock odor in Elav driven *Dgat2 KD* and OE in *App^{NLG} and Aβ42*. **d-e,** Total, day and night sleep (in minutes) and sleep fragmentation in Elav driven *Dgat KD* and OE in *APP/aβ* Models. Two-way ANOVA with multiple comparisons done with Uncorrected Fisher's LSD test was performed for geotaxis, n=3 replicates per group and each group had 10 flies. Chi-square tests were performed for memory assay, *(App^{NLG} N=50, Aβ42=46, W^{1118}=54, GFP=45).* Non-parametric One-way ANOVA with multiple comparisons done with Kruskal Wallis test was performed for sleep activity and sleep fragmentation. Each dot represents several flies *P<0.05, **P<0.01 and ***P<0.001 n.s = not significant. Exact p values are provided in the source data.

Fig.6

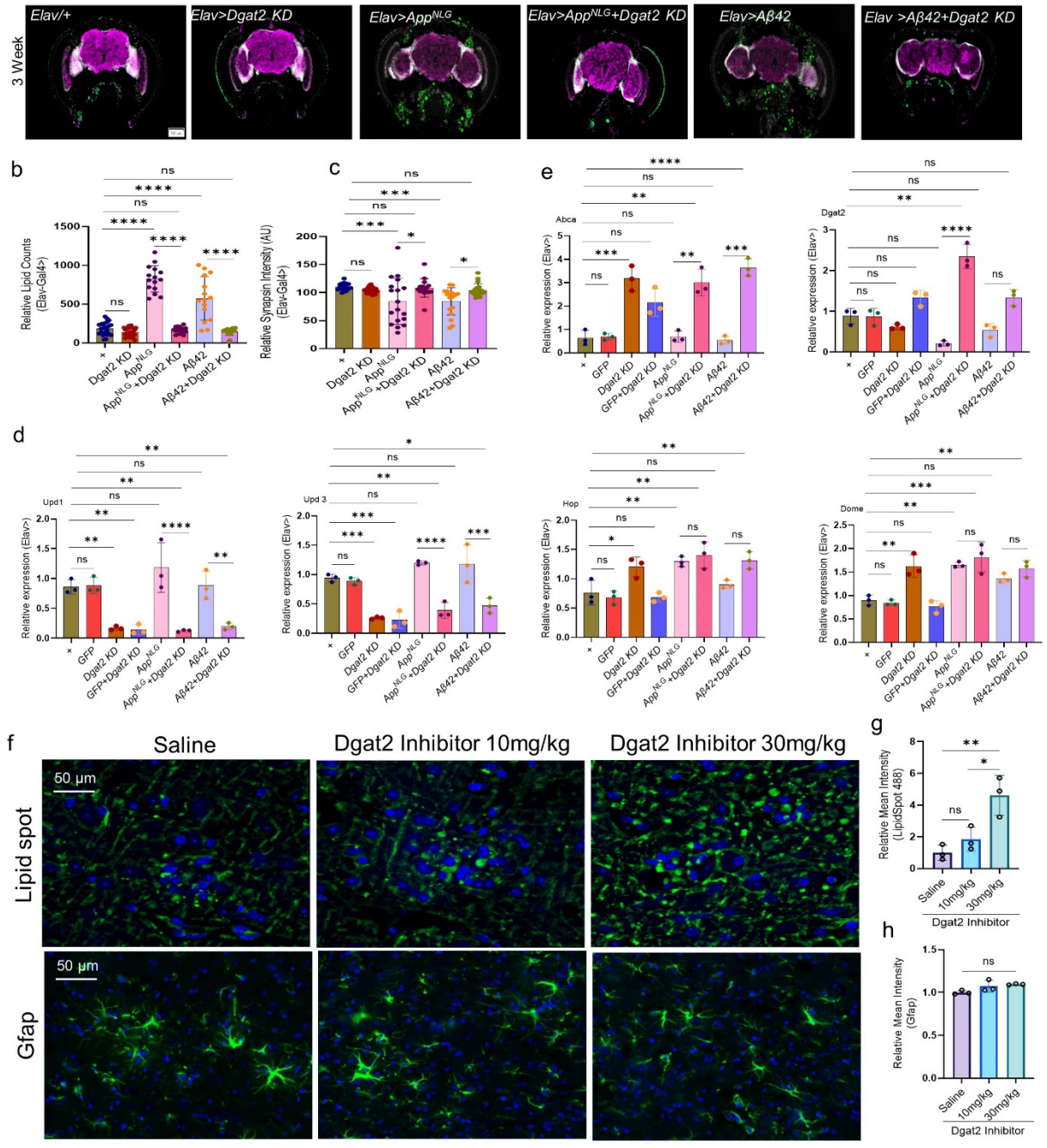
a
3 Week
Elav/+
Elav>Dgat2 KD
Elav>App^NLG
Elav>App^NLG+Dgat2 KD
Elav>Aβ42
Elav >Aβ42+Dgat2 KD
b
Relative Lipid Counts (Elav-Gal4>)
c
Relative Synapsin Intensity (AU) (Elav-Gal4>)
e
Abca
Dgat2
Relative expression (Elav>)
d
Upd1
Upd 3
Hop
Dome
Relative expression (Elav>)
*
Dgat2 KD
App^NLG
App^NLG +Dgat2 KD
Aβ42
Aβ42+Dgat2 KD
GFP
GFP+Dgat2 KD

f
Saline
Dgat2 Inhibitor 10mg/kg
Dgat2 Inhibitor 30mg/kg
Lipid spot
Gfap
50 μm
g
Relative Mean Intensity (LipidSpot 488)
Saline
10mg/kg
30mg/kg
Dgat2 Inhibitor
h
Relative Mean Intensity (Gfap)
Saline
10mg/kg
30mg/kg
Dgat2 Inhibitor

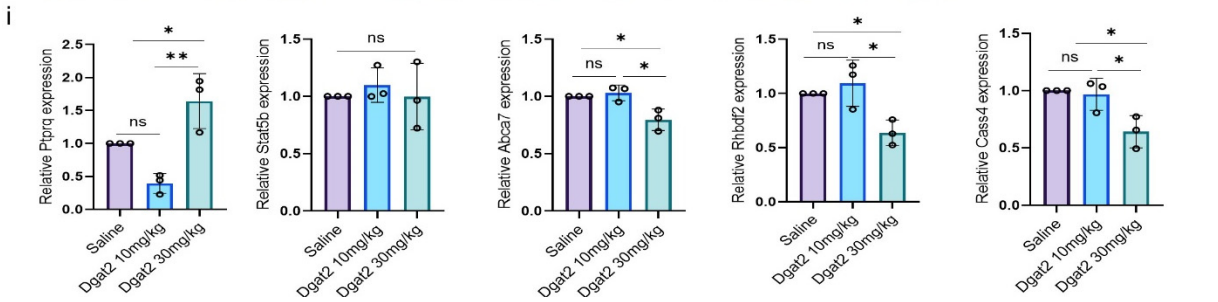
i
Relative Ptprq expression
Relative Stat5b expression
Relative Abca7 expression
Relative Rhbdf2 expression
Relative Cas4 expression
Saline
Dgat2 10mg/kg
Dgat2 30mg/kg

Fig.6| *Dgat2 KD* suppresses lipid metabolism, restores synaptic loss, reduces inflammation in *App^{NLG} and Aβ42* models of *Drosophila*, and modulates AD risk genes and microglial activation in *App^{NLG-F}* mice. a, Representative image showing the expression of lipid accumulation (green), synaptic loss (purple), a marker of neurodegeneration, and DAPI (white) in the brains of Elav-driven KD in AD models in flies**. b-c,** Quantification of the expression level of lipid counts and synapsin intensity in Elav-driven AD models. **d,** Relative expression of inflammatory genes. **e,** Relative expression of metabolic genes in flies. **f,** Immunofluorescence staining showing the expression level of lipid spots and Gfap in hippocampus region of the brain of WT and *App^{NLG-F}* mouse model in presence of Dgat2 inhibitor. **g,** Quantification of the Lipid spot expression level, **h,** Quantification of the Gfap expression level n=3 mice per group. **i,** Relative expression level of inflammatory and AD risk genes WT and App knock-in mouse models in the presence of Dgat2 inhibitor. One-way ANOVA with Turkey's multiple comparisons test was performed for Flies data. N=3 replicates per group and each group has 8-10 flies. Two-way ANOVA with multiple comparisons done with Uncorrected Fisher's LSD test was performed. *$p < .05$; **$p < .01$; ***$p < .001$; ns = not significant. Exact p values are provided in the source data.

Fig.7

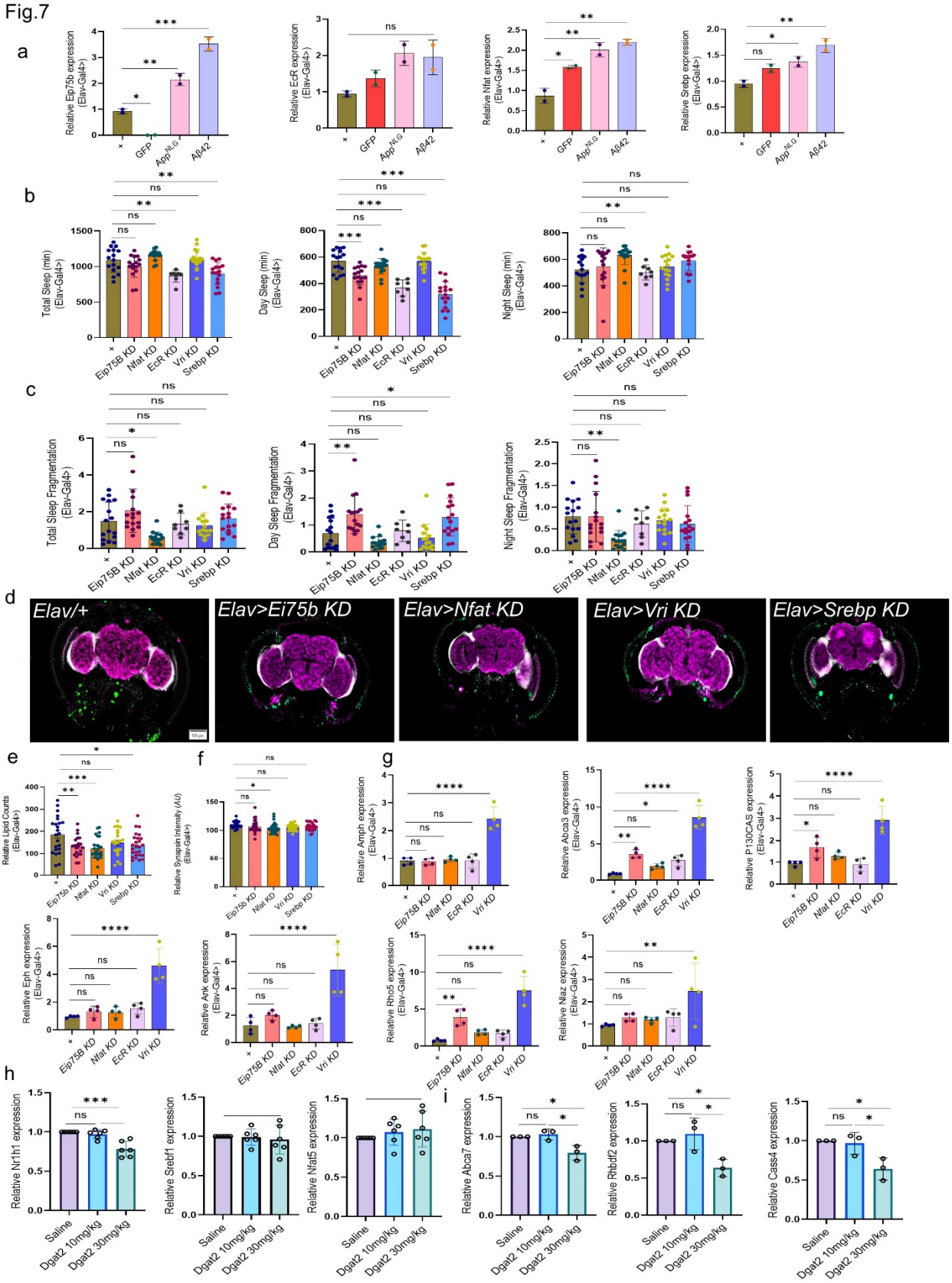
a
Relative Eip75b expression (Elav-Gal4>)
Relative EcR expression (Elav-Gal4>)
Relative Nfat expression (Elav-Gal4>)
Relative Srebp expression (Elav-Gal4>)
+
GFP
App^NLG
Aβ42
b
Total Sleep (min) (Elav-Gal4>)
Day Sleep (min) (Elav-Gal4>)
Night Sleep (min) (Elav-Gal4>)
Eip75B KD
Nfat KD
EcR KD
Vri KD
Srebp KD
c
Total Sleep Fragmentation (Elav-Gal4>)
Day Sleep Fragmentation (Elav-Gal4>)
Night Sleep Fragmentation (Elav-Gal4>)
d
Elav/+
Elav>Ei75b KD
Elav>Nfat KD
Elav>Vri KD
Elav>Srebp KD
e
Relative Lipid Counts (Elav-Gal4>)
Relative Eph expression (Elav-Gal4>)
f
Relative Synapsin Intensity (AU) (Elav-Gal4>)
Relative Ank expression (Elav-Gal4>)
g
Relative Amph expression (Elav-Gal4>)
Relative Abca3 expression (Elav-Gal4>)
Relative P130CAS expression (Elav-Gal4>)
Relative Rho5 expression (Elav-Gal4>)
Relative Nlaz expression (Elav-Gal4>)
h
Relative Nr1h1 expression
Relative Srebf1 expression
Relative Nfat5 expression
i
Relative Abca7 expression
Relative Rhbdf2 expression
Relative Cass4 expression
Saline
Dgat2 10mg/kg
Dgat2 30mg/kg

Fig.7| Dgat2 transcription factor KD alters sleep activity, reduces lipid accumulation, and modulates AD risk genes in Drosophila and inhibition of Dgat2 led to reduced AD risk genes in *App^{NLG-F}* mice. a Relative Dgat2 transcription factors expressions level in Elav-driven *App^{NLG} and Aβ42*. **b,** Total, day and night sleep (minutes) and sleep fragmentation in Elav-driven Dgat2 TFs KD models. **c,** Representative image showing the expression of lipid accumulation (green), synaptic loss (purple), a marker of neurodegeneration, and DAPI (white) in the brains of Elav-driven Dgat2 TFs KD models**. d-e,** Quantification of the expression level of lipid counts and synapsin intensity in Elav-driven Dgat2 TFs KD models**. f,** Relative expressions level of AD risk genes in Elav driven Dgat2 TFs KD models. **g-h,** Relative expressions level of Dgat2 TFs and AD risk genes in App knock-in mouse model in presence of Dgat2 inhibitors. One-way ANOVA with Turkey's multiple comparisons test was performed for Flies data. N=3 replicates per group and each group has 8-10 flies. n=3 mice per group. Two-way ANOVA with multiple comparisons done with Uncorrected Fisher's LSD test was performed in mouse data. *p < .05; **p < .01; ***p < .001; ns = not significant. Exact p values are provided in the source data.

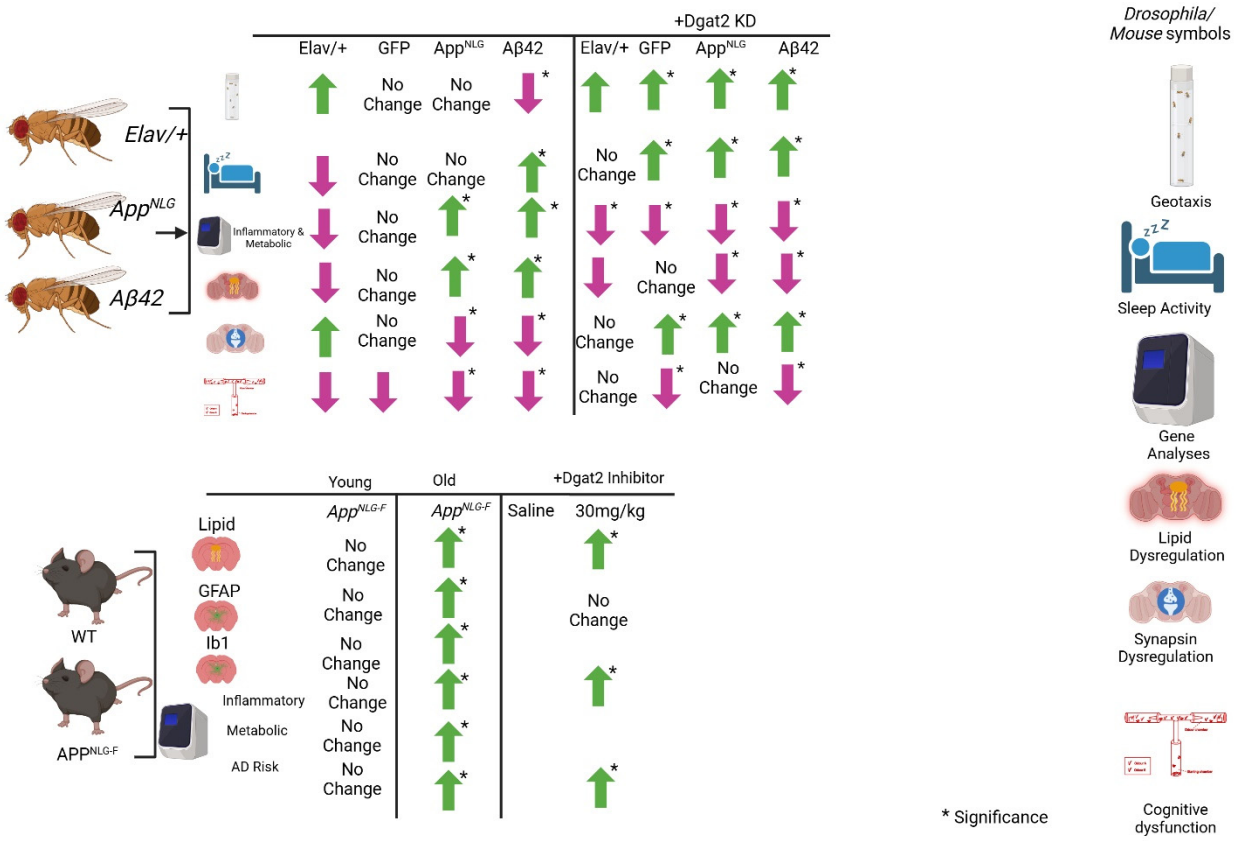

Fig.8. Schematic diagram

Graphical illustration showed the impacts of panneuronal and glial specific expression of *App^{NLG} and Aβ42* without and with *Dgat2 KD* in Drosophila and microglial/ astrocytic activation and lipid accumulation in *App^{NLG-F}* mouse model. The top panel result shows that panneuronal and glial-specific expression of *App^{NLG} and Aβ42* led to compromised locomotor and cognitive performance. It also led to enhanced lipid accumulation and reduced synapsin level, which were further rescued with *Dgat2 KD* (up and down arrows). The bottom panel shows the changes in Gfap, Ib1, Dgat2 stain, and Adrp protein in young/old and with Dgat2 inhibitors in *APP^{NLG-F}* mouse model.